


Landau diamagnetic response in metals as a Fermi surface effect

A. V. Nikolaev

Skobeltsyn Institute of Nuclear Physics, Moscow State University, Vorob'evy Gory 1/2, 119234 Moscow, Russia
 and *Department of Problems of Physics and Energetics, Moscow Institute of Physics and Technology, 141700 Dolgoprudny, Russia*

 (Received 31 August 2018; revised manuscript received 6 November 2018; published 14 December 2018)

It is demonstrated that the Landau diamagnetism of the free electron gas and a monovalent metal can be considered as a Fermi surface effect. Only a relatively small number of electron states close to the Fermi surface are diamagnetically active whereas the majority of the electron states inside the Fermi surface are diamagnetically inert. This partitioning of the occupied electron states is driven by the structure of Landau levels, around which one can introduce magnetic tubes in the reciprocal space. Completely filled magnetic tubes do not change their energy in an applied magnetic field, and only partially occupied magnetic tubes in the neighborhood of the Fermi surface exhibit a diamagnetic response. Using this partitioning of the occupied electron states we derive a general expression for the steady diamagnetic susceptibility, for calculation of which one needs to know the shape of the Fermi surface and the energy gradient on it. The method is applied to alkali metals, whose Fermi surfaces and energy gradients have been obtained from *ab initio* band structure calculations. It has been found that the Landau diamagnetic susceptibility is anisotropic depending on the direction of the applied magnetic field with respect to the Fermi surface. This effect is more pronounced for Li and Cs, whose Fermi surfaces show a noticeable deformation from the spherical shape. The method opens a route for *ab initio* calculations of the Landau diamagnetism of metals or intermetallic compounds. In the case of free electron gas it is shown that this approach also fully describes the oscillatory de Haas–van Alphen part of the diamagnetic susceptibility. Small oscillations of the Fermi energy found in the model are caused by redistribution (inflow or outflow) of electrons from the equatorial region of the Fermi surface.

DOI: [10.1103/PhysRevB.98.224417](https://doi.org/10.1103/PhysRevB.98.224417)

I. INTRODUCTION

When an external magnetic field H is applied to a metallic solid it induces a closed (orbital) motion of the itinerant electrons resulting in a net nonvanishing magnetization antiparallel to H , which we call the Landau diamagnetism [1]. In general the Landau diamagnetic susceptibility χ_L of solids is small and independent of the temperature. In addition to the steady diamagnetism, at very low temperatures and strong magnetic fields there are oscillatory dependencies (χ_{dHvA}) due to the well-known de Haas–van Alphen effect [2–5].

Despite many efforts in the past, an effective method for *ab initio* calculations of the Landau diamagnetism even within the single-electron paradigm has not been established [6,7]. (As summarized in Ref. [6]: “The problem of the low field susceptibility of electrons is old, interesting, and, unfortunately, quite complicated.”) This is because the effect is very difficult from the technical point of view. Even the derivation of this effect for the free electron gas formulated by Landau [1] is rather complex.

In his pioneer work Peierls [8] was the first who extended the Landau treatment to the case of electron band energy law $E(\vec{k})$ within the tight binding approximation. (Alternative derivations were proposed by Wilson [9], Hebborn and Sondheimer [10], and recently by Briet *et al.* [11].) Peierls obtained an expression for the magnetic susceptibility consisting of three terms,

$$\chi = \chi_1 + \chi_2 + \chi_3, \quad (1)$$

where χ_1 is the diamagnetic susceptibility analogous to that of isolated metal atoms, χ_2 is a term which has no simple physical interpretation, and the term χ_3 at zero temperature is given by

$$\chi_3 = -\frac{e^2}{48\pi^3\hbar^2c^2} \int \left\{ \frac{\partial^2 E}{\partial k_x^2} \frac{\partial^2 E}{\partial k_y^2} - \left(\frac{\partial^2 E}{\partial k_x \partial k_y} \right)^2 \right\} \frac{dS}{\nabla_k E}. \quad (2)$$

Here the integration is taken over the Fermi surface. The term χ_3 was considered as leading in the diamagnetism of conduction electrons [8,9,12]. For a simple band it reduces to the Landau-Peierls expression where in the equation for free electron susceptibility the electron mass is replaced by an effective mass m^* . In principle, Eq. (2) suggests that the diamagnetic effect is due to the Fermi surface electron states. However, this statement cannot be proved or considered rigorous because of the other contributions [like χ_1 , χ_2 in Eq. (1)] [8–10,12]. In Ref. [12] on the basis of the study of the density matrix in the magnetic field Wilson, presenting a refined derivation of Eq. (2), has found that some terms cannot be explicitly evaluated and some are not expressible in terms of derivatives of the band energy. More reservations were added by Adams [13] who claimed that the Landau-Peierls susceptibility was not always the dominant contribution. Kjeldaaas and Kohn [14] further suggested that the Landau-Peierls approximation is valid only in the limit of small electron density. This statement has been proven recently by Briet *et al.* [11] at the mathematical level of accuracy. They have also worked out

all satellite terms which in general accompany Eq. (2) but disappear for small electron density.

The full quantum treatment of band diamagnetism in a real solid is a formidable task for a number of reasons. First, the electron motion in the direction of the magnetic field H differs from the motion in the perpendicular plane. In a solid on the other hand, we deal with the translational symmetry which equally holds in three dimensions. Therefore, on applying the magnetic field to a solid, its translational symmetry becomes broken, and accurate description of electron bands and even their classification within the former first Brillouin zone is impossible [6,15]. In general in the magnetic field operators of crystal translation do not commute [6,15]. An effective magnetic band Hamiltonian can be introduced only when the magnetic flux through any triangle formed by two successive translations is a rational number, when expressed in terms of flux quanta [6,15]. These conditions can be satisfied only for some fields H called rational by defining a superlattice structure with a restored vector translation symmetry but a changed point group symmetry. Superlattice calculations are more demanding because the number of inequivalent atoms in the unit cell is several times larger and the first Brillouin zone is less symmetric. For an arbitrary magnetic field H the problem can be sorted out by approximating it with some close rational magnetic field $H' \approx H$.

Second, although the magnetic coupling is much weaker than the electric interactions including the mean field, it is nevertheless responsible for a complete reconstruction of the energy spectrum. Strictly speaking, we have to calculate new energy values and find new state functions explicitly depending on the value of H and populate them accordingly starting from a state with lowest energy and finishing with states of highest energy (E'_F). In this formulation the task has not been solved. Nevertheless, in the past many bright ideas and nontrivial theoretical studies have been invested in this problem [16–21]. For example, one can start with a nearly free electron gas model assuming that the crystal periodic potential is weak [19,20]. The other, more strict approach requires calculated electron bands $E_n(\vec{k})$ in the absence of the magnetic field. The full magnetic Hamiltonian $\hat{H}(\vec{\Pi})$ is an operator depending on $\vec{\Pi} = \vec{p} + e\vec{A}/c$, whose components do not commute. The operator \hat{H} is a matrix function of $\vec{\Pi}$ with matrix elements depending on the magnetic field. When written in diagonal form it can be sufficient to approximate its diagonal elements by the effective Hamiltonian $E_n(\vec{\Pi})$ obtained by replacing $\hbar\vec{k}$ by the operator $\vec{\Pi}$ in the energy band function $E_n(\vec{k})$. Pursuing this approach one can work out the explicit form of the effective Hamiltonian which does not couple different bands and gives the new energy levels. Although this approximation is considered good for isolated (nondegenerate) electron bands E_n , the procedure is not rigorous. In particular, in its derivation some terms on the order of $(\hbar\omega/E_F)^2 \sim H^2$ are omitted [22].

In the effective Hamiltonian treatment, the general effect of the magnetic field on electron bands [7] is twofold: (1) a gradual transformation of band parameters (2) breaking up into a series of discrete states. The latter effect is apparently a manifestation of emerging Landau levels. In Ref. [7] the method reached the stage where in principle all necessary expressions have been derived for the calculation of χ_L within

a pseudopotential (orthogonalized plane wave) basis set. The core formalism however has turned out to be complicated again and the authors use smallness of pseudopotential to obtain estimates of χ_L for real metals.

Diamagnetic response in a metal can be obtained by methods of quantum field theory [23–25]. In Ref. [23] Fourier components of the induced current are calculated through the evolution of the single-particle density matrix. The orbital susceptibility $\chi_{\text{dia}}(q, \omega)$ is found as a prefactor for q^2 (q is the wave vector, ω is the field frequency). The Landau susceptibility χ_L of free electrons is restored at $\omega = 0$ and $q \rightarrow 0$ as a result of cancellation of two terms which diverge as $1/q^2$. In Refs. [25] and [24] a model of conduction electrons interacting with an electromagnetic field is considered. Of particular interest is the electron interaction via current-current potential arising from the exchange of transverse photons. When Dyson equations for complete two-point correlation functions are solved, the Landau susceptibility appears in the corresponding polarization operator [25]. The diamagnetic response comes from the states at the Fermi surface and in general contains terms with the derivatives of the density of states. For arbitrary dispersion however, such terms cannot be expressed as derivatives of the fermionic energy.

There is another approach to the problem based on the semiclassical treatment of the problem [2–5,26]. For example, it has proven to be highly effective in describing the de Haas–van Alphen oscillatory part of the magnetic susceptibility. Onsager [2] and Lifshitz [3], based on the semiclassical description of the movement of an electron in a magnetic field, showed that the change in $1/H$ is determined by extremal cross sections of the Fermi surface in a plane normal to the magnetic field. A good historical and theoretical review of the effect is given in the book of Shoenberg [4]. Although the de Haas–van Alphen effect can be understood within the quantum theory [1,24], the full quantum consideration is not extended to real crystals and in practice the description of the de Haas–van Alphen oscillations relies on the semiclassical theory [4].

From the semiclassical equations it follows that the component of \vec{k} (in the reciprocal space) parallel to \vec{H} and the electron energy $E(\vec{k})$ are both constants of the electron motion. Therefore, in k space electrons move along curves defined by the intersection of isoenergetic surfaces [$E(\vec{k}) = E_0$] with planes perpendicular to the magnetic field; i.e., the scalar potential associated with the electron mean field in solids is unchanged. This is a reasonable assumption especially in the limit of small magnetic fields $\hbar\omega/E_F \rightarrow 0$, which is the case of our consideration.

Electron movement along a closed trajectory (orbit) is a subject of the quantization conditions, Eqs. (5), (6) below. Although these quantization conditions are familiar from the semiclassical approach, they also can be derived from an equation-of-motion method [26,27]. In this paper we will use this semiclassical approach to obtain a very simple expression for the Landau diamagnetic susceptibility of real metals at zero temperature (although the method can be extended to the case of a finite temperature). The elementary unit in our approach is a magnetic tube of finite width and length, containing a certain Landau level inside it. The occupied tubes whose electron states are completely filled are diamagnetically inert.

Only partially occupied tubes located in the neighborhood of the Fermi surface contribute to the diamagnetic effect.

Two important consequences follow from our approach. First, at zero temperature the Landau diamagnetic susceptibility is caused by electron states near the Fermi energy. It is worth noting that the oscillatory part of the diamagnetic susceptibility giving rise to the de Haas–van Alphen effect has been related to the extremal orbits of the Fermi surface for many years. Here we accomplish the relation by ascribing also the steady diamagnetism to the Fermi surface states. The leading role of the Fermi surface in diamagnetism is in accord with the other properties of conduction electrons (for example, the Pauli paramagnetism) which also depend on the peculiarities of electron states near the Fermi energy [28]. Second, the presented method can be applied to *ab initio* calculations of the steady diamagnetic susceptibility of real metals. In this paper we consider the simplest case, which is the case of monovalent alkali metals. We hope that in principle based on our simple expression (55) below, the Landau susceptibility can be added to a list of physics quantities available from first-principles calculations.

We should also mention the important question of the Fermi energy (E_F) change in the applied magnetic field. This is a very weak effect, considered first in detail by Kaganov *et al.* [29]. Some consequences of the phenomenon including weak oscillations of the density of states at the Fermi level are further discussed by Shoenberg in Ref. [4]. Below we will unveil a mechanism of this effect for the free electron gas case. It is caused by peculiarities of electron population in the equatorial region of the Fermi sphere. Depending on the applied magnetic field there can be a small inflow or outflow of electrons from the equatorial region to other states of the Fermi surface.

The paper is organized as follows. In Sec. II we demonstrate the method for the free electron gas. There, we introduce a central object for our method—a magnetic tube—and consider its properties. The most important one is that the tube whose electron states are completely occupied does not contribute to magnetic response. Then we select diamagnetically active tubes near the Fermi surface and calculate their steady diamagnetic susceptibility χ_L . The oscillatory (de Haas–van Alphen) contribution (χ_{dHvA}) is considered in Sec. II D. Here the analytical calculations become more involved although the general physical picture remains clear and transparent. The description of the steady diamagnetism of real metals, Sec. III, follows the same lines. As in the case of the Fermi gas, we first consider magnetic tubes of real systems and then calculate their steady diamagnetic response. The application of the method for calculations of χ_L for various magnetic field directions is given in Sec. IV. Finally, in Sec. V we summarize the main conclusions.

II. FREE ELECTRON GAS

A. Magnetic tubes in \vec{k} space

In an external magnetic field \vec{H} directing along the z axis, the energy of the free electron is given by [1]

$$E = \hbar\omega\left(n + \frac{1}{2}\right) + \frac{\hbar^2 k_z^2}{2m}, \quad (3)$$

where n is integer (numbering the Landau levels), k_z is the z component of the wave vector \vec{k} , and the cyclotron frequency

$$\omega = \frac{eH}{mc}. \quad (4)$$

Here m and e are the electron mass and charge; c is the speed of light. In correspondence with Eq. (3) the energy of the electron is presented by two contributions, the contribution E_\perp from the movement in the plane, perpendicular to \vec{H} [i.e., in the plane (k_x, k_y)], and the contribution $E_z = \hbar^2 k_z^2 / 2m$ from the movement parallel to \vec{H} (i.e., along the z axis). In the following we consider only the component E_\perp , because the parallel component $E_\parallel = E_z$ is unchanged in the magnetic field.

Although Eq. (3) is obtained within the fully quantum treatment, below we will follow the widely used semiclassical representation of electron orbits in the real and momentum ($\hbar\vec{k}$) space [2,3,5,26], which gives exactly the same energy spectrum. The electron movement in the magnetic field in the (x, y) plane along the radial direction $q = r$ or along the $q = x$ or y axis (depending on the choice of the vector potential gauge) is described by a quantized orbit,

$$\oint p_q dq = 2\pi\hbar(n + \gamma), \quad (5)$$

which corresponds to the n th Landau level with the factor γ . In the Wentzel, Kramers, and Brillouin (WKB) method for nonsingular integrable orbits $\gamma = \mu/2$ [26], where μ is the Maslov index. In our case $\mu = 2$ and $\gamma = 1/2$ [26]. In the (k_x, k_y) momentum plane the electron orbit defined by Eq. (5) is visualized as a circle whose area A_n is given by

$$A_n = \frac{2\pi eH}{c\hbar} \left(n + \frac{1}{2}\right), \quad (6)$$

and its energy is

$$E_{\perp,n} = \hbar\omega\left(n + \frac{1}{2}\right). \quad (7)$$

It is well known that the average density of electron states in the \vec{k} space remains the same as without magnetic field. To understand better the reconstruction of the electron structure in the magnetic field H , we select in the \vec{k} space a tube whose number of electron states and in which the energy of all states do not change in the presence of H , Fig. 1. For that we consider auxiliary electron orbits of the area

$$A_n^{\text{aux}} = \frac{2\pi eH}{c\hbar} n \quad (8)$$

with energies

$$E_n^{\text{aux}} = \hbar\omega n. \quad (9)$$

Note the the n th Landau orbit defined by Eqs. (6), (7) is situated between the auxiliary orbits n and $n + 1$, Fig. 1 (left panel), and its energy E_n lies between E_n^{aux} and E_{n+1}^{aux} . Below we show that the number of electron states with energies $E_n^{\text{aux}} \leq E \leq E_{n+1}^{\text{aux}}$ without field equals the number of electron states condensing on the n th Landau level in the presence of the field. The same holds for their total energies.

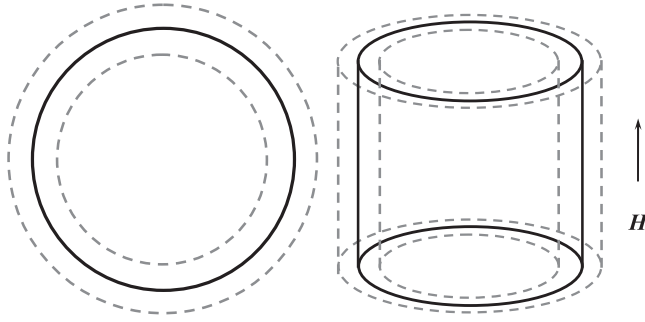


FIG. 1. Magnetic tube and the corresponding Landau level. On the left: The (k_x, k_y) tube cross section and the n th Landau orbit (the solid circle with the in-plane energy E_n). The dashed circles correspond to the auxiliary orbits with energies E_n^{aux} and E_{n+1}^{aux} . On the right: The tube in the \vec{k} space. Without magnetic field electron states are distributed throughout the whole tube; in the presence of field, only on the Landau orbit in the middle.

For that we calculate the density of electron states \mathcal{N}_\perp in the (k_x, k_y) plane,

$$\mathcal{N}_\perp = \frac{dN_\perp}{dE_\perp} = \frac{2m}{\hbar^2} \frac{L_x L_y}{2\pi}, \quad (10)$$

and notice that \mathcal{N}_\perp is independent of the energy E_\perp . (Here L_x , L_y , and L_z are distances of the free electron gas box in x , y , and z directions, respectively.) Using (10), we find the number of electron states in the n th tube without field, i.e., in the energy range $E_n^{\text{aux}} \leq E \leq E_{n+1}^{\text{aux}}$,

$$\Delta N_n(H=0) = \int_{E_n^{\text{aux}}}^{E_{n+1}^{\text{aux}}} \mathcal{N}_\perp dE_\perp = \mathcal{N}_\perp \hbar\omega = 2N_p. \quad (11a)$$

Here N_p is the spatial degeneracy of the Landau levels (without spin polarization),

$$N_p = \frac{L_y}{2\pi} \frac{m\omega}{\hbar} L_x = \frac{L_x L_y eH}{2\pi c\hbar}. \quad (11b)$$

Calculating the total energy of these states without field,

$$\begin{aligned} \mathcal{E}_n(H=0) &= \int_{E_n^{\text{aux}}}^{E_{n+1}^{\text{aux}}} \mathcal{N}_\perp E_\perp dE_\perp \\ &= \frac{1}{2} [(E_{n+1}^{\text{aux}})^2 - (E_n^{\text{aux}})^2] \mathcal{N}_\perp = E_{\perp,n} \Delta N_n, \end{aligned} \quad (11c)$$

we find that it coincides with the energy of all electron tube states condensed on the n th Landau level in the presence of the field. Thus, we have proven that

$$\Delta N_n(H=0) = \Delta N_n(H \neq 0) = 2N_p, \quad (12a)$$

$$\mathcal{E}_n(H=0) = \mathcal{E}_n(H \neq 0) = \hbar\omega(n + \frac{1}{2})2N_p. \quad (12b)$$

So far our consideration has been limited by the (k_x, k_y) plane. However, since Eqs. (12a) and (12b) hold for any k_z component, they are fulfilled for the whole tube n , Fig. 1. In other words, if without field, a tube contains electron states which satisfy the inequality $E_n^{\text{aux}} \leq E_\perp \leq E_{n+1}^{\text{aux}}$ for all k_z in the range $k_z^{(1)} \leq k_z \leq k_z^{(2)}$, then in the presence of the magnetic field all these states condense on the n th Landau level, that is, $E_\perp(k_z) = E_{\perp,n}(k_z)$ throughout the k_z region, Fig. 1.

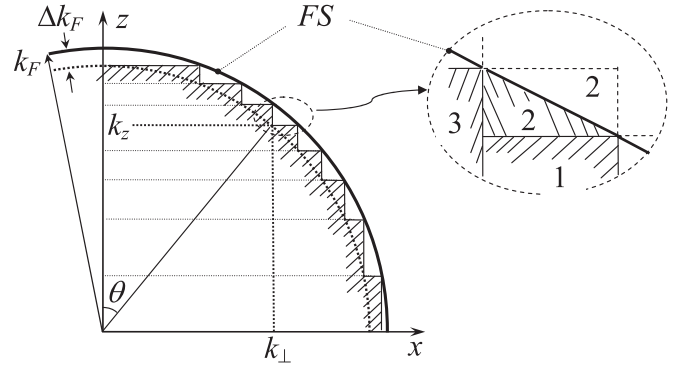


FIG. 2. Magnetic tubes and the Fermi surface (FS); the (k_x, k_z) cross section in the \vec{k} space. The tubes inside the Fermi sphere, shown as dashed area on the left panel, are completely filled and diamagnetically inert. Inset: 1, completely occupied tube n ; 2, partially occupied tube n ; 3, completely occupied tube $(n-1)$.

Furthermore, the total electron energy of the tube remains unchanged, which bears some resemblance to the Bohr–van Leeuwen theorem in classical physics. The upper $k_z^{(2)}$ and lower $k_z^{(1)}$ boundary of the tube can be taken as arbitrary. For practical reasons for each tube n we define the k_z boundary by its intersection with the Fermi surface, Fig. 2. We then obtain two n th tubes: the first tube (denoted by 1 in the inset of Fig. 2) lies entirely inside the Fermi surface and being completely occupied does not exhibit diamagnetism. The second tube (denoted by 2 in the inset of Fig. 2) being only partially filled below the Fermi surface results in a diamagnetic response. We consider this effect in the following sections.

It is also worth noting that the \vec{k} -space partitioning depends on the value of the magnetic field, since $\omega \sim H$, and the tube boundaries are defined by ω , Eq. (9).

B. Diamagnetically active electron states

Consider the Fermi surface and define necessary magnetic tubes parallel to the z axis (in the direction of the magnetic field H), Fig. 2, as discussed in Sec. II A. Boundary conditions defined by in-plane circular orbits, Eq. (8), specify a set of concentric cylindrical surfaces, which intersect the Fermi surface in circles perpendicular to the z axis. We then draw the planes of the circles and use them to construct a set of tubes, limited by the planes and the cylindrical surfaces, which lie inside the Fermi sphere. The (k_x, k_z) cross section of these tubes is schematically shown in Fig. 2. The fully occupied tubes are shown as the dashed area. The electron states of the completely filled tubes do not change their energy in a magnetic field. Therefore, the whole effect is due to the states lying in the partially occupied tubes. Their cross sections in the (k_x, k_z) plane look like a chain of triangles, Fig. 2.

Consider a typical partially occupied tube, whose triangle cross section in the (k_x, k_z) plane is shown in Fig. 3. We denote two legs of the triangle by Δk_\perp and Δk_z . Taking into account that the area of the (k_x, k_y) cross section of the n th tube is $\Delta A = A_{n+1}^{\text{aux}} - A_n^{\text{aux}} = 2\pi eH/c\hbar$, and that $\hbar\omega \ll E_F$, we obtain

$$\Delta k_\perp = \frac{\Delta A}{2\pi k_\perp} = \frac{m\omega}{\hbar k_F \sin \theta}. \quad (13)$$

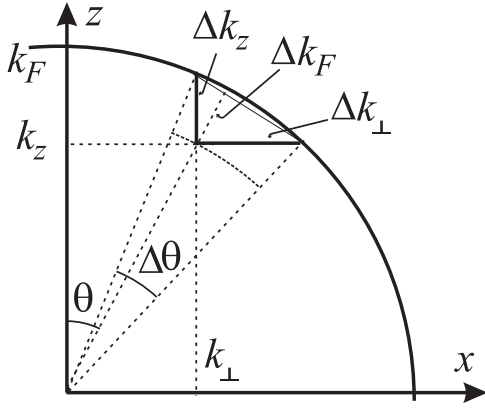


FIG. 3. A typical (k_x, k_z) cross section of a partially occupied tube near the Fermi surface. The triangle size is greatly exaggerated, since $\Delta k_F = m\omega/\hbar k_F \ll k_F$.

(Here Θ is the polar angle, Figs. 2, 3.) Therefore, the narrow surface region of the partially occupied tube is defined by the wave vector quantity Δk_F shown in Figs. 2 and 3,

$$\Delta k_F = \Delta k_{\perp} \sin \Theta = \frac{m\omega}{\hbar k_F}. \quad (14)$$

It is remarkable that Δk_F is independent of Θ . Therefore, the radius $k_F - \Delta k_F$ determines an auxiliary internal sphere in the \vec{k} space, which can be used for drawing the stepwise line shown in Figs. 2 and 3, separating the fully occupied tubes from the partially occupied ones.

For the angle $\Delta\Theta$ shown in Fig. 3, we obtain

$$\Delta\Theta = \frac{\Delta k_F}{k_F} \frac{1}{\cos \Theta \sin \Theta}. \quad (15)$$

Notice, that Eq. (13) has a singularity at $\Theta = 0$, and Eq. (15) at $\Theta = 0$ and $\pi/2$. Therefore, the polar and equatorial region of the Fermi sphere should be considered more attentively; see Sec. IID below.

Now we find the number of active electron states in the partially occupied tubes,

$$N = \sum_{n=1}^M \Delta N_n, \quad (16)$$

where $\Delta N_n \equiv \Delta N(k_z, k_z + \Delta k_z)$ is the number of the electron states in the n th partially filled tube, whose k_z component lies between $k_{z,n} \equiv k_z$ and $k_{z,n+1} \equiv k_z + \Delta k_z$. Using the infinitesimal property of the (k_x, k_y) cross section we find

$$\Delta N = 2v\Delta V_k = 2\pi v \frac{eH}{\hbar c} \Delta k_z, \quad (17)$$

where ΔV_k is the volume of the partially occupied tube in k space and $v = V/(2\pi)^3$ (in the general case ΔN is calculated in Appendix A).

Notice that from Eq. (17) it follows that $\Delta N/\Delta k_z = \text{constant}$. Furthermore, $\Delta N/\Delta k_z$ is independent of m , which will be fully appreciated in the general case considered below in Sec. IIIB. Since for usual magnetic fields $\Delta k_F, \Delta k_z \ll k_F$, in Eq. (16) we can substitute the summation with the

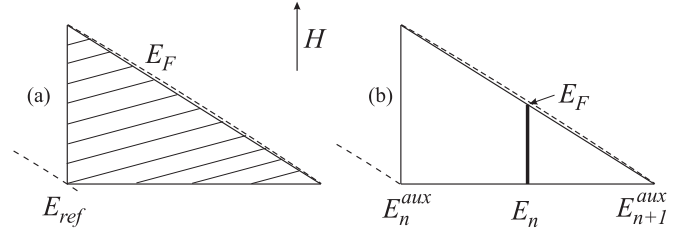


FIG. 4. The (k_x, k_z) cross section of a partially occupied tube near the Fermi level. On the left (a): Dashed area shows the occupied electron states without magnetic field, $\vec{H} = 0$. On the right (b): Bold vertical line shows the occupied electron states (1D gas) in the magnetic field $\vec{H} \neq 0$. E_F is the Fermi energy of the one-dimensional electron gas (along the z axis), whose transverse energy E_n is determined by the n th Landau energy.

integration

$$N = \int dN = \int_{k_z^{\min}}^{k_z^{\max}} \left(\frac{\Delta N}{\Delta k_z} \right) dk_z. \quad (18)$$

For the free electron gas $k_z^{\min} = -k_F$, $k_z^{\max} = k_F$. Using (17), (18) we arrive at

$$N = 2\pi v \frac{eH}{\hbar c} \ell_z, \quad (19)$$

where $\ell_z \equiv k_z^{\max} - k_z^{\min} = 2k_F$ is defined exclusively by the projection of the Fermi surface along the direction of the applied magnetic field. Therefore, $N \sim H$. Since the perturbation energy for each electron state can be estimated with $\hbar^2 k_F \Delta k_F / m = \hbar\omega \sim H$, the total energy change in the magnetic field $\sim H^2$, which leads to the constant magnetic susceptibility χ . (The rigorous computation of χ is given in the next section.)

C. Steady diamagnetic susceptibility

A remarkable property of partially occupied tubes near the Fermi surface is that application of a magnetic field does not lead to electron transitions between different tubes (with the exception of a small number of electrons in the equatorial region). Therefore, upon applying the field, there is a redistribution of electron states only within each partially filled tube.

To demonstrate this, we consider in detail the transformation of electron states in the tube n when the magnetic field is switched on. [Without field the number of electron states ΔN is given by Eq. (17).] The occupation of electron states for two cases ($H = 0$ and $H \neq 0$) is shown schematically in Fig. 4. When $H \neq 0$, all electrons of the tube are on the n th Landau level with the transverse energy E_n , and occupy the lowest k_z states, as shown in Fig. 4. If all electrons remain in the tube, then the highest energy level with the wave vector δk_z (with respect to k_z of the n th tube, Fig. 3) is found from the following relation:

$$2\delta k_z N_p l_z = \Delta N. \quad (20)$$

We recall that N_p is the in-plane (or transverse) folding of the n th Landau level, while $l_z = L_z/2\pi$ is the density of electron states along k_z . Substituting in Eq. (20) Eq. (11b) for N_p and

Eq. (17) for ΔN , we obtain

$$\delta k_z = \frac{1}{2} \Delta k_z. \quad (21)$$

(The result for the infinitely small triangle cross section can be foreseen from the geometrical reasons.)

Equation (21) leads to an important consequence. The energy of the highest occupied electron level coincides with E_F and the wave vector k_F lies on the Fermi surface even in the applied magnetic field $H \neq 0$. Since the conclusion holds for all partially occupied tubes (with the exception of few equatorial tubes), the highest energy of the occupied electron states, E_F , is conserved as the Fermi energy for all tubes and there are no electron transitions between tubes. (The exceptional case of the equatorial region is considered later in Sec. II D.) Therefore, in the following we can calculate the energy change for each tube separately.

Keeping in mind that in the magnetic field there are two energy contributions— E_\perp in the (k_x, k_y) plane and E_z at k_z —we obtain for the energy change of the partially filled tube n

$$\Delta E = \Delta E_\perp^{H \neq 0} + \Delta E_z^{H \neq 0} - \Delta E^{H=0}. \quad (22)$$

The notation Δ on the right-hand side is an indication that the corresponding energy refers to the partially filled tube n , whose k_z values are in the range from $k_{z,n}$ to $k_{z,n+1} = k_{z,n} + \Delta k_z$, Fig. 2, 3. The quantities $\Delta E_\perp^{H \neq 0}$, $\Delta E_z^{H \neq 0}$, and $\Delta E^{H=0}$ therefore refer to energy components of the tube with ($H \neq 0$) and without ($H = 0$) magnetic field.

The detailed simple calculations of all components are performed in Appendix B (with respect to the energy E_{ref} , Fig. 4). As a result, we get

$$\frac{\Delta E^{H=0}}{\Delta N} = \frac{2}{3} \frac{\hbar^2}{m} k_F \Delta k_F = \frac{2}{3} \hbar \omega \quad (23)$$

for the energy components without magnetic field and

$$\frac{\Delta E_\perp^{H \neq 0}}{\Delta N} = \frac{1}{2} \hbar \omega, \quad (24a)$$

$$\frac{\Delta E_z^{H \neq 0}}{\Delta N} = \frac{1}{4} \hbar \omega \quad (24b)$$

in the applied magnetic field. In fact, taking into account that ΔN stands for the number of electrons, the right-hand sides of Eqs. (23), (24a), and (24b) represent average energy values independently of the tube under consideration. The substitutions of Eqs. (23), (24a), and (24b) in Eq. (22) yields

$$\Delta E = \frac{1}{12} \hbar \omega \Delta N > 0. \quad (25)$$

Note that Eq. (25) refers to any partially filled tube. Therefore, making the summation over all tubes and using Eq. (19) with $\ell_z = 2k_F$, we find

$$E = \frac{1}{12} \hbar \omega N = \frac{1}{3} \pi v k_F \frac{e^2 H^2}{m c^2}. \quad (26)$$

For the magnetic susceptibility χ we finally have

$$\chi = -\frac{d^2 E(H)}{dH^2} = -\frac{2}{3} \pi v k_F \frac{e^2}{m c^2} = -\frac{e^2 k_F V}{12 \pi^2 m c^2}. \quad (27)$$

This is the celebrated expression obtained by Landau for the diamagnetic susceptibility of the free electron gas.

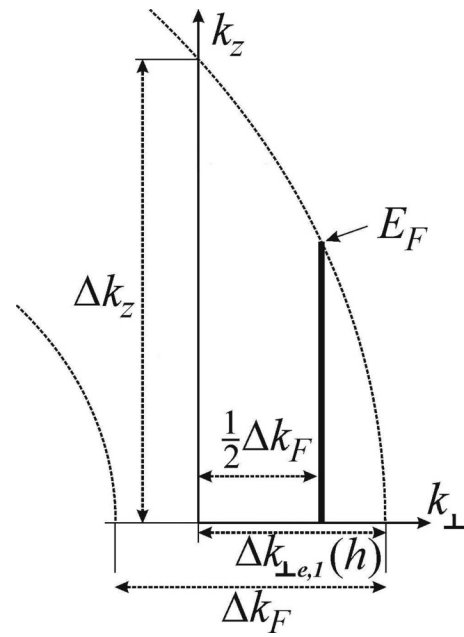


FIG. 5. First equatorial tube. Landau states (shown by the bold line) are occupied if $\Delta k_{\perp,e,1} = h > \Delta k_F/2$ (or $r > 1/2$), and empty if $h < \Delta k_F/2$ ($r < 1/2$).

D. Oscillatory (equatorial) diamagnetic susceptibility

Earlier (Sec. III C) we have obtained the diamagnetic effect based on calculations of the energy of active electrons in the partially occupied tube of general form. Deviations from the general situation are possible for boundary cases, which are the polar region ($\Theta = 0$) with the Landau level $n = 0$, and the equatorial region ($\Theta = \pi/2$). In Appendix C we analyze the polar region and show that it complies with the general case. In the equatorial region however the situation is very different.

The problem is that the stepwise line shown in Fig. 2 can terminate at the equatorial point with $\Theta = \pi/2$ in any place with $k_{\perp,e}$ lying in the interval $k_F - \Delta k_F \leq k_{\perp,e} \leq k_F$, and the equatorial point does not necessarily lie on the internal sphere of the radius $k_F - \Delta k_F$, which is the case for all other tubes, Fig. 5. This equatorial tube is truncated because its upper energy boundary E_{n+1}^{aux} , defined by (9), in general lies outside the (k_x, k_y) equatorial cross section of the Fermi sphere and cannot be reached. We define this irregular tube with $k_\perp \geq k_{\perp,e}$ as the first equatorial tube. Notice that when $k_{\perp,e} \rightarrow k_F$, the area of the (k_x, k_z) cross section of this tube approaches zero. In that case one has to resort to the preceding tube (that is, with $k_\perp < k_{\perp,e}$), which also makes an irregular contribution to energy. We define it as the second equatorial tube. The other tubes essentially follow the general dependencies considered in Sec. III C.

For the first equatorial tube we define the quantity $\Delta k_{\perp,e,1} = k_F - k_{\perp,e}$, Fig. 5, for which we shall also use a short notation $h = \Delta k_{\perp,e,1}$. The subscripts $e, 1$ and $e, 2$ refer to the first and second equatorial tubes, respectively. As discussed above, h ranges from 0 to Δk_F . Consider the important dimensionless parameter

$$r = \frac{h}{\Delta k_F}. \quad (28)$$

Clearly, $0 < r < 1$. Note that by varying H we change the structure of all magnetic tubes, and, consecutively the parameter r , defined by the geometry of the last tube. Therefore, r implicitly depends on H . It can be shown that in a first approximation r is proportional to $1/H$.

For $\Delta k_{z,e,1}$ we obtain

$$\Delta k_{z,e,1} = \sqrt{2k_F h} = \sqrt{2r \frac{eH}{\hbar c}}. \quad (29)$$

Calculating the number of states in the first equatorial tube without magnetic field, we find

$$\Delta N_{e,1}^{H=0} = \frac{8\pi}{3} r v \frac{eH}{\hbar c} \Delta k_{z,e,1}. \quad (30)$$

Based on the analysis of the Cornu spiral sum, Pippard estimated that the relative weight of the extremal region should be $\Delta N_e/N \sim \sqrt{H}$ (Eq. (33) of Ref. [30]). This conclusion is in agreement with Eq. (30) since $\Delta N_{e,1}^{H=0}/N \sim \Delta k_{z,e,1} \sim \sqrt{\omega} \sim \sqrt{H}$.

Notice that already in obtaining $\Delta N_{e,1}^{H=0}$ we have a deviation from the general case, Eq. (30), and

$$\frac{\Delta N_{e,1}^{H=0}}{\Delta \Theta_{e,1}} = \frac{4r}{3} \frac{\Delta N}{\Delta \Theta}. \quad (31)$$

Here $\Delta \Theta_{e,1}$ defines the angular size of the first equatorial triangle in the (k_x, k_z) cross section. Deviations are also present for the transverse and z energy contributions.

Now we consider the situation in the magnetic field $H \neq 0$. We start as in Sec. III C with finding the wave vector δk_z of the highest occupied electron state along the z axis under assumption that all electrons belonging to the first equatorial tube do not leave it. By means of Eq. (20) we get

$$\delta k_{z,e,1} = \frac{2}{3} r \Delta k_{z,e,1}. \quad (32)$$

Now however the energy of the highest occupied state in general differs from E_F , and therefore from the energy of the highest occupied states in other tubes, Eq. (21). Below we consider the situation for two different cases: $0 \leq r < 1/2$ (case *a*) and $1/2 \leq r < 1$ (case *b*).

In case *a* the energy of the Landau level of the first equatorial tube $E_n - E_{\text{ref}}^{e,1} = \hbar\omega/2$, Fig. 5, is higher than E_F even at $k_z = 0$. Therefore, all electrons from this tube move to other tubes where they occupy free states above E_F . As a result, a small rise in E_F should occur, but since $\Delta N_{e,1} \ll N$, it is on the order of $\hbar\omega \Delta N_{e,1}/N \ll \hbar\omega$. Since $E_F - E_{\text{ref}}^{e,1} = r\hbar\omega$, the energy of the promoted electrons is $\Delta E^{H \neq 0, a} / \Delta N_{e,1}^{H=0} = r\hbar\omega$ (with respect to $E_{\text{ref}}^{e,1}$).

In case *b* the Landau level at $k_z = 0$ lies below E_F and in the magnetic field it becomes partially occupied by electrons with $k_z > 0$. The maximal z -wave vector δk_F^z of the 1D electron state lying on the Fermi sphere can be found by requiring its energy to be equal to E_F ,

$$\delta k_F^z = \sqrt{2k_F \left(h - \frac{1}{2} \Delta k_F \right)} = \Delta k_{z,e,1} \sqrt{\frac{r - \frac{1}{2}}{r}}. \quad (33)$$

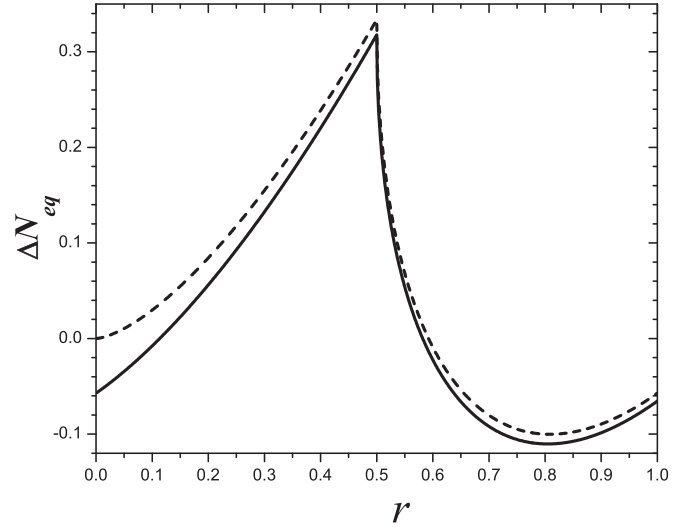


FIG. 6. The number of electrons [in units of $8\pi v(eH/\hbar c)^{3/2}$] promoted from the equatorial range to other tubes, $\Delta N_{eq} = \Delta N_e^{H=0} - \Delta N_e^{H \neq 0}$, expressed in terms of the dimensionless parameter $r \sim 1/H$. Negative values imply that electrons move to the equatorial tube. The dashed line stands for the contribution from the first equatorial tube; the solid line, from the first and second equatorial tubes. The same plot [in units of $(eH/\hbar c)^{3/2} \hbar^2 / mk_F$] describes a small oscillatory dependence of the Fermi energy (chemical potential).

The number of the occupied electron states in the tube, $\Delta N_{e,1}^{H \neq 0, b}$, is determined by

$$\frac{\Delta N_{e,1}^{H \neq 0, b}}{\Delta N_{e,1}^{H=0}} = \frac{3}{2r^{3/2}} \sqrt{r - \frac{1}{2}}. \quad (34)$$

The condition $\Delta N_{e,1}^{H=0} > \Delta N_{e,1}^{H \neq 0, b}$ in terms of r means $1/2 \leq r < \sqrt{3} \sin \pi/9$, while $\Delta N_{e,1}^{H=0} \leq \Delta N_{e,1}^{H \neq 0, b}$ results in $\sqrt{3} \sin \pi/9 \leq r < 1$. Therefore, if $1/2 \leq r < 0.529$, electrons from the first equatorial tube partially move to other (regular) tubes as happens in case *a*. For $0.529 \leq r < 1$ the opposite happens, that is, a small number of electrons from all regular tubes move to the equatorial tube. The change of the number of electrons in the equatorial region is shown in Fig. 6.

To single out the irregular contribution explicitly, we rewrite it in the following form,

$$E = E_L + \Delta E_{eq}. \quad (35)$$

Here E_L is the diamagnetic (regular) contribution, Eq. (26), and ΔE_{eq} stands for the irregular term from the equatorial region. If only the first equatorial tube is accounted for, then $\Delta E_{eq} = \Delta E_{eq,1}$, where

$$\begin{aligned} \Delta E_{eq,1} = & \Delta E_{\perp, e,1}^{H \neq 0} + \Delta E_{z, e,1}^{H \neq 0} - \Delta E_{e,1}^{H=0} \\ & + \Delta E_{pr,1} - \Delta E_{\text{corr},1}. \end{aligned} \quad (36)$$

Here $\Delta E_{pr,1}$ is the energy of the promoted electrons (transferred to or from regular tubes), while $\Delta E_{\text{corr},1}$ stands for the

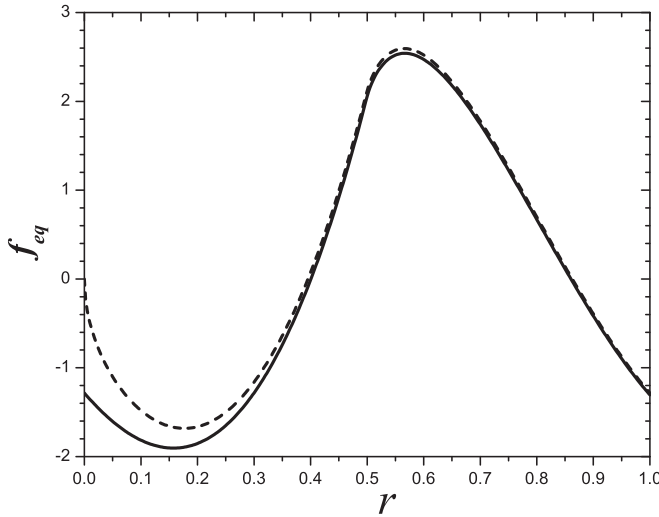


FIG. 7. The oscillatory behavior of the irregular contribution to energy, $\Delta E_{eq} \sim f_{eq}(r)$, from the equatorial region, expressed in terms of the dimensionless parameter $r \sim 1/H$. The dashed line stands for the contribution from the first equatorial tube; the solid line, from the first and second equatorial tubes.

regular diamagnetic contribution of the equatorial region,

$$\frac{\Delta E_{corr,1}}{\Delta N_{e,1}^{H=0}} = \frac{1}{16r} \hbar \omega. \quad (37)$$

Collecting all energy terms together, we arrive at

$$\Delta E_{eq} = 2 \frac{m\pi v}{15\sqrt{2}} \omega^2 \sqrt{\frac{m}{\hbar}} \omega f_{eq}(r). \quad (38)$$

(The factor 2 stands for two equivalent contributions from the upper and lower Fermi semisphere.) For the first equatorial tube we have $f_{eq}(r) = f_{eq,1}(r)$, and the function $f_{eq,1}(r)$ has different dependencies for cases *a* and *b*, described earlier. In case *a* ($0 \leq r < 1/2$) $f_{eq,1}(r) = f_{eq,1}^a(r)$,

$$f_{eq,1}^a(r) = \sqrt{r} (32r^2 - 5); \quad (39a)$$

in case *b* ($1/2 \leq r < 1$) $f_{eq,1}(r) = f_{eq,1}^b(r)$,

$$f_{eq,1}^b(r) = \sqrt{r} (32r^2 - 5) - 80(r - \frac{1}{2})^{3/2}. \quad (39b)$$

The dependence of $\Delta E_{eq,1} \sim f_{eq,1}(r)$ on r is shown in Fig. 7. Note that $\Delta E_{eq,1}(r=0) \neq \Delta E_{eq,1}(r=1)$, although $r=0$ and $r=1$ refer to the same physical situation. Below we shall see that by including two equatorial tubes, the equality of the energy at $r=0$ and $r=1$ is restored.

In calculating the magnetic susceptibility χ_{eq} one has to keep in mind that ΔE_{eq} depends on H through ω explicitly and on r implicitly. It can be shown that the contribution from the derivative of $r(H)$ with respect to the magnetic field H is dominant. Finally, we obtain

$$\chi_{eq} = -\frac{\sqrt{2}m\pi v}{15} \omega^2 \sqrt{\frac{m}{\hbar}} \omega \frac{\partial^2 f_{eq}(r)}{\partial r^2} \left(\frac{\partial r}{\partial H} \right)^2. \quad (40)$$

The plot of $\chi_{eq}(r)$ is reproduced in Fig. 8. It is worth noting that $\chi_{eq,1}$ diverges at $r \rightarrow 0^+$ (the divergence disappears when the second equatorial tube is accounted for) and at $r \rightarrow$

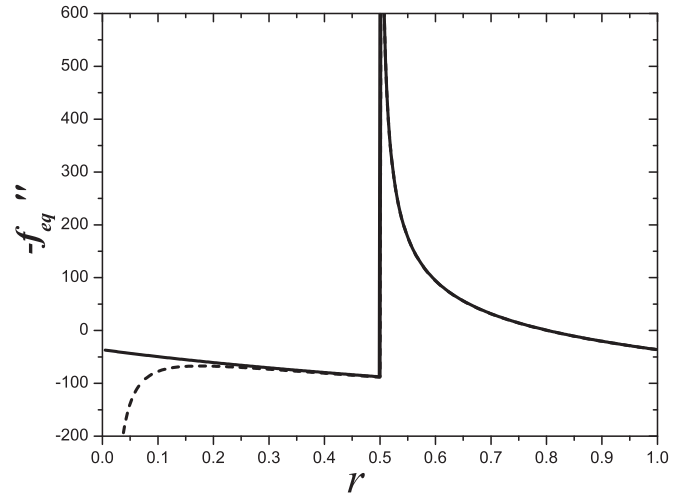


FIG. 8. The oscillatory dependence of the magnetic susceptibility $\chi_{eq} \sim -f''_{eq}(r)$ from the equatorial region expressed in terms of the dimensionless parameter $r \sim 1/H$ (see text). The dashed line stands for the contribution from the first equatorial tube; the solid line, from the first and second equatorial tubes.

$(1/2)^+$. The latter persists in a more refined calculation with two or more equatorial tubes, because it is connected with the onset of the occupation of a new Landau level in the (k_x, k_y) equatorial plane.

Notice that if we limit ourselves to the case of only the first equatorial tube, then in correspondence with Eqs. (39a) and (39b), the energy values at $r=0$ and $r=1$ are different, namely $\Delta E_{eq,1}(0) = 0$, $\Delta E_{eq,1}(1) \neq 0$, Fig. 7. In reality the physical situation is the same; the condition $r=0$ simply implies that the first equatorial tube is absent, while the second equatorial tube plays the role of the first. The inconsistency exists for the other quantities, for example, for the magnetic susceptibility, Fig. 8. Therefore, to make the values at $r=0$ and $r=1$ consistent, we have to take into account the irregular term from the second equatorial tube. Then the contribution from the equatorial region ΔE_{eq} , described by (38), changes,

$$\Delta E_{eq} = \Delta E_{eq,1} + \Delta E_{eq,2}, \quad (41)$$

and the function $f_{eq}(r)$ in (38) becomes

$$f_{eq}(r) = f_{eq,1}(r) + f_{eq,2}(r). \quad (42)$$

Numerical results for two equatorial tubes are shown by solid lines in Figs. 6, 7, and 8. It is worth noting that except for the range around $r=0$ and $r=1$, the inclusion of the second equatorial tube plays only a minor role.

III. MONOVALENT METAL

A. Magnetic tubes and their properties

In an externally applied magnetic field \vec{H} pointing along the z axis, the energy spectrum of the occupied electron states of real metals is completely changed. Here and below we follow the semiclassical representation of electron orbits in the real and momentum ($\hbar\vec{k}$) space as briefly described in Sec. II A. It is worth mentioning that the semiclassical picture

for itinerant electrons has been supported by the equation-of-motion method of Ref. [27], provided that in the quantization condition, Eq. (5), $\gamma = 1/2 + \hbar\Gamma_1 + \hbar^2\Gamma_3 \approx 1/2$ (here $\hbar = eH/c$). Notice however that in the limit of small magnetic field $\hbar \rightarrow 0$ and $\gamma \rightarrow 1/2$. Therefore, in the following we will still use $\gamma = 1/2$, although this is not critical for the method; see details in Appendix D.

In the momentum space the n th Landau orbit in the (k_x, k_y) plane is defined by the area A_n Eq. (6), and the orbital motion is associated with the energy $E_{\perp,n}$, Eq. (7). The real-space orbit defined by Eq. (5) is no longer a circle, but a closed curve corresponding to the \vec{k} orbit in the (k_x, k_y) plane rotated through $\pi/2$ about the field direction and scaled by $\hbar c/eH$. In real metals, in contrast to the free electron gas, Eq. (D4), the cyclotron frequency ω is given by

$$\omega = \frac{eH}{cm^*}, \quad (43)$$

where the effective cyclotron mass m^* is defined as

$$m^* = \frac{\hbar^2}{2\pi} \frac{\partial A}{\partial E}. \quad (44)$$

Here A is the area of the electron orbit in the (k_x, k_y) plane of the \vec{k} space. In practice, $\partial A/\partial E$ is found from the contour integral

$$\frac{\partial A}{\partial E} = \oint \frac{dk}{\left| \left(\frac{\partial E}{\partial \vec{k}} \right)_{\perp} \right|}. \quad (45)$$

From Eq. (45) we conclude that in general for different Landau levels n and m with energies $E_n \neq E_m$ we have $(\partial A/\partial E)_n \neq (\partial A/\partial E)_m$ and consequently $m_n^* \neq m_m^*$, $\omega_n \neq \omega_m$. For real metals for neighboring Landau levels like n and $n' = n \pm 1$ since $\hbar\omega \ll E_F$ we still have $m_n^* \approx m_m^*$, $\omega_n \approx \omega_m$.

So far, it has been implied that $k_z = 0$. Since k_z is a constant of the electron motion [5], we can easily extend our consideration to the general case with $k_z \neq 0$ as has been done in Sec. II A for the free electron gas. The most important difference with the Fermi gas is that the quantities A_n , $\partial A/\partial E$, and hence m^* and ω depend on k_z . Thus, in general the total electron energy is given by

$$E = E_{\perp,n} + E_z(k_z), \quad (46)$$

where $E_z(k_z)$ is the electron energy associated with the one-dimensional (1D) electron band describing the electron motion in the z direction. Notice that at $k_z = 0$ we have $E_z = 0$. Therefore, in general $E_z(k_z) = E(\vec{k}) - E_{\perp,n}(\vec{k})$, provided that \vec{k} lies on the Landau level n . In the free electron case $E_z(k_z) = \hbar^2 k_z^2/2m$.

As in the case of the Fermi gas, we select in the \vec{k} space a tube whose main property will be that its number of electron states and energy of all states do not change in the presence of the external magnetic field. At each component k_z we consider auxiliary quantized electron orbits O_n with areas

$$A_n^{\text{aux}} = \frac{2\pi eH}{c\hbar} (n + \delta) \quad (47)$$

in the (k_x, k_y) plane, where $\delta \sim H$ is a small parameter ($\delta \ll 1$) which is discussed in detail in Appendix D. Its choice is

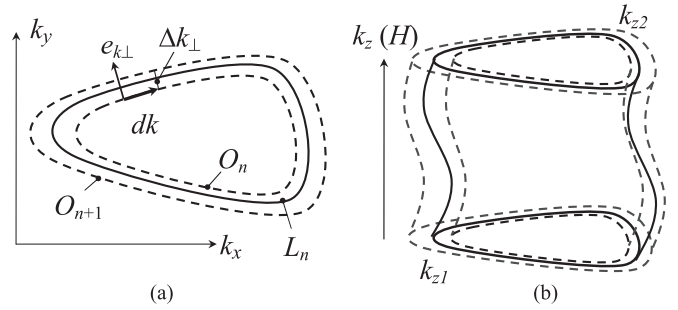


FIG. 9. Magnetic tube and the corresponding Landau level. On the left (a): The (k_x, k_y) tube cross section and the n th Landau level (the solid line L_n). The dashed circles correspond to two auxiliary quantized orbits: O_n and O_{n+1} ; see text for details. On the right (b): The tube in the \vec{k} space, $k_{z1} \leq k_z \leq k_{z2}$. Without magnetic field electron states are distributed throughout the whole tube; in the presence of field, they are condensed on the Landau level in the middle.

determined by imposing the equality of energy [see Eq. (51b) below] to a very high accuracy. At fixed value of H , A_n^{aux} is a constant area throughout k_z although the shape of the orbit can vary with k_z . We associate with A_n^{aux} a certain energy of the electron movement in the (k_x, k_y) plane, which we denote as E_n^{aux} . At $k_z = 0$ this energy coincides with the orbital band energy, i.e., $E_n^{\text{aux}} = E(\vec{k})$, where \vec{k} lies on the O_n orbit. For $k_z \neq 0$ using the proximity to $E_{\perp,n}$ we have $E_n^{\text{aux}} \approx \hbar\omega(n + \delta)$, Appendix D.

Note that at any fixed k_z the n th Landau level L_n whose area is given by Eq. (6) is sandwiched between auxiliary orbits O_n and O_{n+1} , Eq. (47), as shown in Fig. 9. Moreover, for a band with dispersion the Landau energy $E_{\perp,n}$, Eq. (7), lies between E_n^{aux} and E_{n+1}^{aux} . Since $E_{n+1}^{\text{aux}} - E_n^{\text{aux}} \approx \hbar\omega \ll E_F$, within the interval $(A_n^{\text{aux}}, A_{n+1}^{\text{aux}})$ between the auxiliary orbits n and $n + 1$ we deal with an infinitesimal situation. Below we show that in the (k_x, k_y) plane the number of electron states with energies $E_n^{\text{aux}} \leq E \leq E_{n+1}^{\text{aux}}$ without magnetic field equals the number of electron states condensing on the n th Landau level in the presence of the field. The same holds for their total energy. We start by noting that the density of electron states $\mathcal{N}_{\perp}(E)$ in the (k_x, k_y) plane is

$$\mathcal{N}_{\perp}(E_{\perp}) = \frac{dN_{\perp}}{dE_{\perp}} = 2 \frac{L_x L_y}{(2\pi)^2} \frac{\partial A}{\partial E} = \frac{2m^*}{\hbar^2} \frac{L_x L_y}{2\pi}. \quad (48)$$

(Here the double spin degeneracy is taken into account.) Using Eqs. (48) and (44), we find that the number of electron states in the n th tube without field, i.e., in the energy range $E_n^{\text{aux}} \leq E \leq E_{n+1}^{\text{aux}}$, is

$$\begin{aligned} \Delta N_n(H = 0) &= \int_{E_n^{\text{aux}}}^{E_{n+1}^{\text{aux}}} \mathcal{N}_{\perp}(E_{\perp}) dE_{\perp} \\ &= \frac{2L_x L_y}{(2\pi)^2} (A_{n+1}^{\text{aux}} - A_n^{\text{aux}}) = 2N_p, \end{aligned} \quad (49)$$

where N_p is the spatial degeneracy of the Landau levels, Eq. (11b). Calculating the energy of these states without field

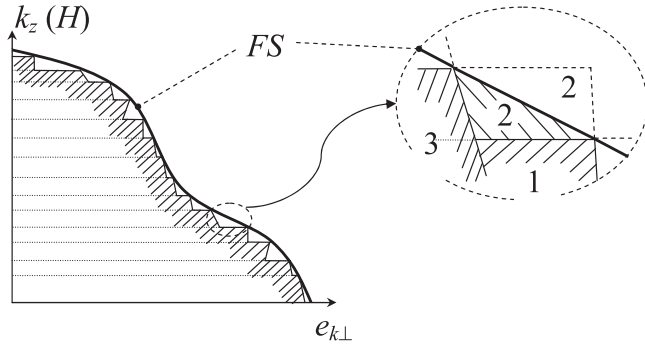


FIG. 10. Magnetic tubes and the Fermi surface (FS) in a magnetic field in the (k_z, e_{k_\perp}) cross section in the \vec{k} space. All electron states within the tubes inside the Fermi surface, shown as the dashed area on the left, are completely filled, and their full energy does not change in the magnetic field. The diamagnetic effect is due to the electron states of partially occupied tube states (like tube 2 in the inset), making a steplike structure near the Fermi surface. Inset: 1, completely occupied tube n ; 2, partially occupied tube n ; 3, completely occupied tube $n - 1$.

to an accuracy of $(\hbar\omega/E_F)^3 \Delta N_n$, Appendix D, we obtain

$$\mathcal{E}_n(H = 0) = \int_{E_n^{\text{aux}}}^{E_{n+1}^{\text{aux}}} \mathcal{N}_\perp(E_\perp) E_\perp dE_\perp = E_{\perp,n} \Delta N_n. \quad (50)$$

That is, $\mathcal{E}_n(H = 0)$ coincides with the energy of these states on the n th Landau level in the presence of the field. Thus, we have proven that

$$\Delta N_n(H = 0) = \Delta N_n(H \neq 0) = 2N_p, \quad (51a)$$

$$\mathcal{E}_n(H = 0) = \mathcal{E}_n(H \neq 0) = \hbar\omega(n + \frac{1}{2})2N_p. \quad (51b)$$

Equations (51a) and (51b) are valid for any k_z component, and therefore for the whole tube n , Fig. 9, defined by its upper $(k_z^{(2)})$ and lower $(k_z^{(1)})$ boundaries, $k_z^{(1)} \leq k_z \leq k_z^{(2)}$. As for the free electron gas, $k_z^{(2)}$ and $k_z^{(1)}$ are conveniently defined by the intersection of a tube with the Fermi surface, Fig. 10. As a result, we have two n th tubes: the first tube (denoted by 1 in the inset of Fig. 10) lies entirely inside the Fermi surface and does not exhibit diamagnetism, while the second tube (denoted by 2 in the inset of Fig. 10) is only partially filled and results in a diamagnetic response. We consider this effect in the following sections.

B. Diamagnetically active electron states

Consider the Fermi surface and define magnetic tubes in an externally applied magnetic field H pointing in the positive z direction, Fig. 10. As has been discussed in Sec. III A, each magnetic tube n at k_z is sandwiched between two boundary electron orbits O_n and O_{n+1} in the (k_x, k_y) plane whose areas A_n^{aux} and A_{n+1}^{aux} are defined by Eq. (47). As a result we obtain a set of boundary surfaces that intersect the Fermi surface in orbits perpendicular to the z axis. The intersection orbits unlike simple circles for the Fermi gas, Sec. II, are rather complicated, and below we describe them in detail. These orbits lie in (k_x, k_y) planes and we can use them to define two k_z boundary conditions, $k_z^{(n,1)}$ and $k_z^{(n,2)}$, in such a way that the magnetic tube n lies entirely inside the Fermi surface.

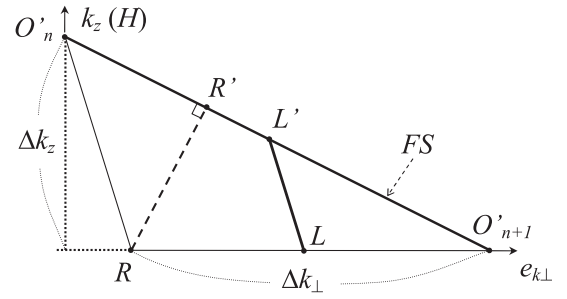


FIG. 11. The (k_z, e_{k_\perp}) cross section of a partially occupied tube n near the Fermi surface. FS stands for the Fermi surface, LL' for Landau orbits L_n , O'_n and O'_{n+1} for auxiliary quantized orbits. R is the energy reference point, $E_{\text{ref}} = E(R) = E_F - \hbar\omega$, $E(L) = E_{\text{ref}} + \hbar\omega/2$, $\Delta l_F = |O'_n O'_{n+1}|$, $\Delta k_F = |RR'|$.

The fully occupied tubes are schematically shown in Fig. 10. In Sec. III A we have seen that the electron states of the completely filled tubes do not change their energy in magnetic field. Therefore, the whole effect is due to the states lying in the partially occupied tubes passing through the Fermi surface (like tube 2 in the inset of Fig. 10).

Consider a boundary orbit $O_{n,F}$ [defined by $A_n^{\text{aux}} = \text{constant}$, Eq. (47)] in the (k_x, k_y) plane lying on the Fermi surface. It defines a certain value of k_z which we denote by $k_{z,n}$. The electron energy band gradient, $\partial E(\vec{k})/\partial \vec{k}$, on $O_{n,F}$ is perpendicular to the Fermi surface and hence to the orbit. In addition, we will use the projection of the gradient in the plane of the orbit, $(\partial E/\partial \vec{k})_\perp$, which is also perpendicular to $O_{n,F}$, Figs. 9, 11. The normalized vector in the direction of $(\partial E/\partial \vec{k})_\perp$ will be denoted by e_{k_\perp} . Notice that plane (k_z, e_{k_\perp}) is normal to $O_{n,F}$. Cross sections of magnetic tubes passing through the Fermi surface are schematically shown by horizontal dotted lines in Fig. 10. [In general, Fig. 10 should be understood as composed of many different panels—at most one panel for each tube cross section, because the energy gradient $\partial E/\partial \vec{k}$ and hence (k_z, e_{k_\perp}) planes still can have different orientations.]

Consider a typical partially occupied tube n whose triangle cross section in the (k_z, e_{k_\perp}) plane is shown in Fig. 11. Points O'_n and O'_{n+1} are defined by the intersection of the (k_z, e_{k_\perp}) plane with the orbits $O_{n,F}$ and $O_{n+1,F}$, respectively. The side O'_n, O'_{n+1} is the intersection with the Fermi surface, the side O'_n, R is the intersection with the A_n^{aux} boundary surface, and the side O'_{n+1}, R is the intersection with the (k_x, k_y) plane of the orbit $O_{n+1,F}$. It is convenient to count energy from $E_{\text{ref}} = E(R) = E_F - \hbar\omega$. The vector \vec{RR}' being perpendicular to O'_n, O'_{n+1} is collinear with the energy gradient $\partial E/\partial \vec{k}$. Finally, the line L, L' is given by the intersection of Landau orbits L_n at various k_z , Eq. (6), with the (k_z, e_{k_\perp}) plane. Since we consider the limit of small magnetic fields, i.e., $\hbar\omega/E_F \rightarrow 0$, the triangle is assumed infinitesimal allowing for linear dependencies of relevant quantities. In particular, the line L, L' is parallel to R, O'_n , etc., and we can take $\delta = 0$ in Eq. (47), $\gamma = 1/2$ in Eq. (5), Appendix D.

In the following we will need Δk_\perp , Δk_z , Δk_F expressed in terms of $(\partial E/\partial \vec{k})_F$, $(\partial E/\partial \vec{k}_\perp)_F$, $(\partial A/\partial k_z)_F$ calculated at the Fermi surface. Details of these calculations are given in Appendix A.

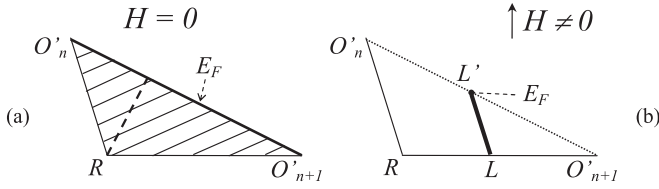


FIG. 12. The (k_z, e_{k_\perp}) cross section of a partially occupied tube n near the Fermi level. On the left (a): Occupied electron states without magnetic field, $\vec{H} = 0$. On the right (b): The occupied electron states on Landau levels (the LL' bold line) in the magnetic field $\vec{H} \neq 0$. E_F is the Fermi energy of the one-dimensional electron states, whose transverse energy E_n is determined by the n th Landau energy, $E_n = E_{n,\perp}(L)$.

Now in accordance with Eq. (16) we can find the number of the active electron states in all partially occupied tubes. We recall that in Eq. (16) $\Delta N_n \equiv \Delta N(k_z, k_z + \Delta k_z)$ is the number of the electron states in the n th partially filled tube, whose k_z component lies between $k_{z,n} \equiv k_z$ and $k_{z,n+1} \equiv k_z + \Delta k_z$. The calculation of ΔN carried out in Appendix A results in Eq. (17), that is,

$$\frac{\Delta N}{\Delta k_z} = 2\pi v \frac{eH}{\hbar c} = \text{constant}. \quad (52)$$

Notice that the right-hand side of Eq. (52) is independent of the effective mass m^* and $\partial A/\partial E$. It should be emphasized that the polar and equatorial regions of the Fermi surface are special cases, which are discussed in Sec. III D. It turns out that the polar regions fully comply with the general expression (52), while the equatorial regions [where $\partial A(k_z)/\partial k_z = 0$] give rise to the well-known de Haas–van Alphen oscillations of the magnetic susceptibility, which is not the subject of the present study.

For small magnetic fields when $\Delta k_z \ll k_F$, in Eq. (16) we can substitute the summation with the integration, Eq. (18). In Eq. (18) k_z^{\min} (k_z^{\max}) is the minimal (maximal) k_z component of the vectors \vec{k} lying on the Fermi surface. Using (52) [or Eq. (17)] we arrive at Eq. (19), where $\ell_z \equiv k_z^{\max} - k_z^{\min}$ is defined exclusively by the projection of the Fermi surface along the direction of the applied magnetic field. Notice however that unlike for free electron gas, now in general $k_z^{\min} \neq -k_F$, $k_z^{\max} \neq k_F$. Furthermore, as discussed later in Sec. IV in real metals ℓ_z depends on the orientation of the applied magnetic field with respect to the Fermi surface.

Thus, the number of active electron states $N \sim H$, their total energy change in the magnetic field $\sim H^2$, which gives a constant diamagnetic susceptibility χ .

C. Landau diamagnetic susceptibility

The transformation of the electron states of a partially occupied tube is schematically shown in Fig. 12. In the applied magnetic field $H \neq 0$ all electrons of the partially occupied tube are on the n th Landau orbits with the transverse energy E_n , and occupy the lowest in energy k_z states, as shown in Fig. 12.

As we have seen in Sec. II C for the free electron gas the highest occupied energy in the presence of the field coincides with the Fermi energy E_F obtained in the absence of the field.

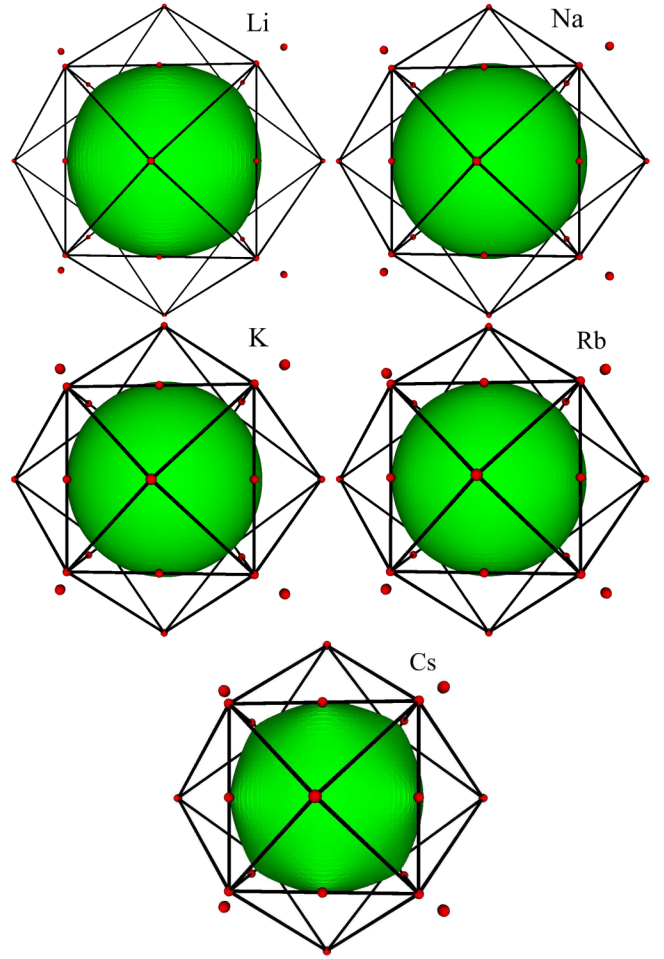


FIG. 13. Calculated Fermi surfaces of alkali metals.

For the real metal the (k_z, e_{k_\perp}) cross section of a partially occupied tube n , Figs. 11 and 12, in general is very different from the (k_z, k_x) cross section of the Fermi gas shown in Figs. 3 and 4. However, the highest occupied energy is still E_F . This follows from Eq. (20), written for the partially occupied tube n for real metal. In terms of the z projection δk_z of the wave vector \vec{k}_L shown in Fig. 11, it implies $\delta k_z = \Delta k_z/2$ just as for the Fermi gas, Eq. (21). Therefore, there are no electron transitions between different tubes and we can calculate the energy change for each tube separately and then sum all contribution for the final result.

Keeping in mind that in the magnetic field there are two energy contributions— E_\perp in the (k_x, k_y) plane and E_z at k_z , Eq. (46)—we now calculate the energy change for the tube n in the applied magnetic field, Eq. (22).

The calculation of all components is performed in Appendix B (with respect to the energy E_{ref} , Fig. 12), and results in Eqs. (23), (24a), and (24b). For the total energy change we get $\Delta E = \hbar\omega \Delta N/12$. This is the same expression as for the free electron gas, Eq. (25), but now the cyclotron frequency ω is different for different tubes, Eq. (43). Therefore, by means of Eqs. (43) and (52) we rewrite the expression for ΔE in terms of Δk_z :

$$\Delta E = \frac{1}{6}\pi v \left(\frac{eH}{c} \right)^2 \frac{\Delta k_z}{m^*}. \quad (53)$$

TABLE I. Calculated characteristics of alkali metals: χ_L is the steady diamagnetic susceptibility (*av* stands for the averaged value), χ_P is the Pauli paramagnetic susceptibility, m^* is the effective cyclotron mass, k_H^{\max} is the maximal projection of the Fermi surface on the direction of the applied magnetic field \vec{H} , γ_{el} is the linear electron specific heat coefficient (in mJ/mole K²), $N(E_F)$ is the electron density of states (in 1/eV). C_l^{FS} ($l = 0, 4, 6, 8$) are the coefficients describing the shape of the Fermi surface and C_l^g are the coefficients of the expansion of the modulus of the energy gradient ($\vec{\nabla}_k E_F$). a is the bcc lattice constant (in Å), and indices [001], [101], or [111] define the direction of \vec{H} , at which the corresponding quantity is calculated; see text for details.

	Li	Na	K	Rb	Cs
a (Å)	3.50	4.29	5.35	5.585	6.14
χ_L^{av} (10^{-7})	-1.753	-2.086	-1.624	-1.515	-1.179
$\chi_L[001]$ (10^{-7})	-1.670	-2.081	-1.631	-1.508	-1.142
$\chi_L[101]$ (10^{-7})	-1.871	-2.090	-1.631	-1.560	-1.308
$\chi_L[111]$ (10^{-7})	-1.714	-2.084	-1.618	-1.485	-1.114
m_{av}^*	1.517	1.036	1.067	1.097	1.300
$m_{av}^*[001]$	1.552	1.038	1.065	1.099	1.310
$m_{av}^*[101]$	1.462	1.035	1.065	1.080	1.214
$m_{av}^*[111]$	1.527	1.037	1.070	1.107	1.317
$k_H^{\max}[001]$	0.576	0.480	0.386	0.369	0.333
$k_H^{\max}[101]$	0.609	0.481	0.386	0.375	0.353
$k_H^{\max}[111]$	0.582	0.481	0.385	0.366	0.326
$N(E_F)$	0.486	0.494	0.792	0.888	1.302
γ_{el}	1.146	1.166	1.867	2.094	3.068
χ_P (10^{-7})	12.207	6.728	5.565	5.487	6.051
C_0^{FS}	2.08862	1.70433	1.36665	1.30909	1.19032
C_4^{FS}	-0.01529	-0.00039	0.00092	-0.00048	-0.00474
C_6^{FS}	-0.02358	-0.00065	-0.00101	-0.00694	-0.02149
C_8^{FS}	0.00660	-0.00001	0.00074	0.00263	0.00914
C_0^g	1.40005	1.64429	1.28035	1.19546	0.94458
C_4^g	0.13752	0.01058	-0.00908	0.00294	0.04106
C_6^g	0.28278	0.01325	0.00441	0.08695	0.24620
C_8^g	-0.10748	-0.00267	-0.00733	-0.05090	-0.12383

Note that Eq. (53) refers to any partially filled tube. Therefore, making the summation over all tubes we find

$$E = \frac{1}{48} \frac{V}{\pi^2} \left(\frac{eH}{c} \right)^2 \int_{k_z^{\min}}^{k_z^{\max}} \frac{dk_z}{m^*(k_z)}. \quad (54)$$

Here, as before, k_z^{\min} (k_z^{\max}) is the minimal (maximal) k_z component of the Fermi surface. Notice that m^* found from Eqs. (44) and (45) for orbits in the (k_x, k_y) plane lying on the Fermi surface is a function of k_z . Finally, for the magnetic susceptibility χ we have

$$\chi = -\frac{d^2 E(H)}{dH^2} = -V \frac{1}{24} \frac{e^2}{\pi^2 c^2} \int_{k_z^{\min}}^{k_z^{\max}} \frac{dk_z}{m^*(k_z)}. \quad (55)$$

In the case of the free electron gas the integral on the right-hand side of (55) is reduced to $\ell_z/m = 2k_F/m$ and we arrive at Eq. (27) for the diamagnetic susceptibility of the Fermi gas. In general, Eq. (55) differs from the pioneer expression of Peierls [8], Eq. (2), although for the case of parabolic bands in terms of k_x and k_y , Eq. (E1), they give identical results, Appendix E.

As a final and important remark we note that the density of electron states, $g(E_F)$, remains unchanged on applying the magnetic field, although energy gradients at the Fermi surface change their directions and values. We prove this remarkable effect in Appendix F.

D. Special cases and extremal cross sections of the Fermi surface

General expressions for Δk_{\perp} and Δk_z , Eqs. (A1) and (A2), become indefinite when $(\partial E/\partial \vec{k})_{\perp} = 0$ or $\partial A/\partial k_z = 0$. The condition $(\partial E/\partial \vec{k})_{\perp} = 0$ occurs at polar points of the Fermi surface and the full account of this situation is given in Appendix C. In that case there are no deviations from the general final equations (52) and (53).

If $\partial A(k_z)/\partial k_z = 0$ then from Eq. (A2) it follows that $\Delta k_z \rightarrow \infty$, and such an extremal cross section corresponds to a maximum or a minimum of $A(k_z)$ as a function of k_z . It is well known that extremal orbits and extremal regions give rise to the oscillatory behavior for the diamagnetic response (de Haas–van Alphen effect), Ref. [4]. In our approach for the Fermi gas described in detail in Sec. IID, it has also been demonstrated that the extremal region consisting of a few tubes in the equatorial region of the Fermi surface results in the oscillatory behavior of the diamagnetic susceptibility. This should occur in real metals as well, but in this paper we consider only the regular contribution to energy (ΔE_{eq}^L) leaving the irregular part (ΔE_{eq}^{irr}) for future consideration.

IV. APPLICATION TO ALKALI METALS

We have applied the method to calculations of the diamagnetic response of alkali metals: Li, Na, K, Rb, and Cs, which are crystallized in the body centered cubic (bcc) lattice and

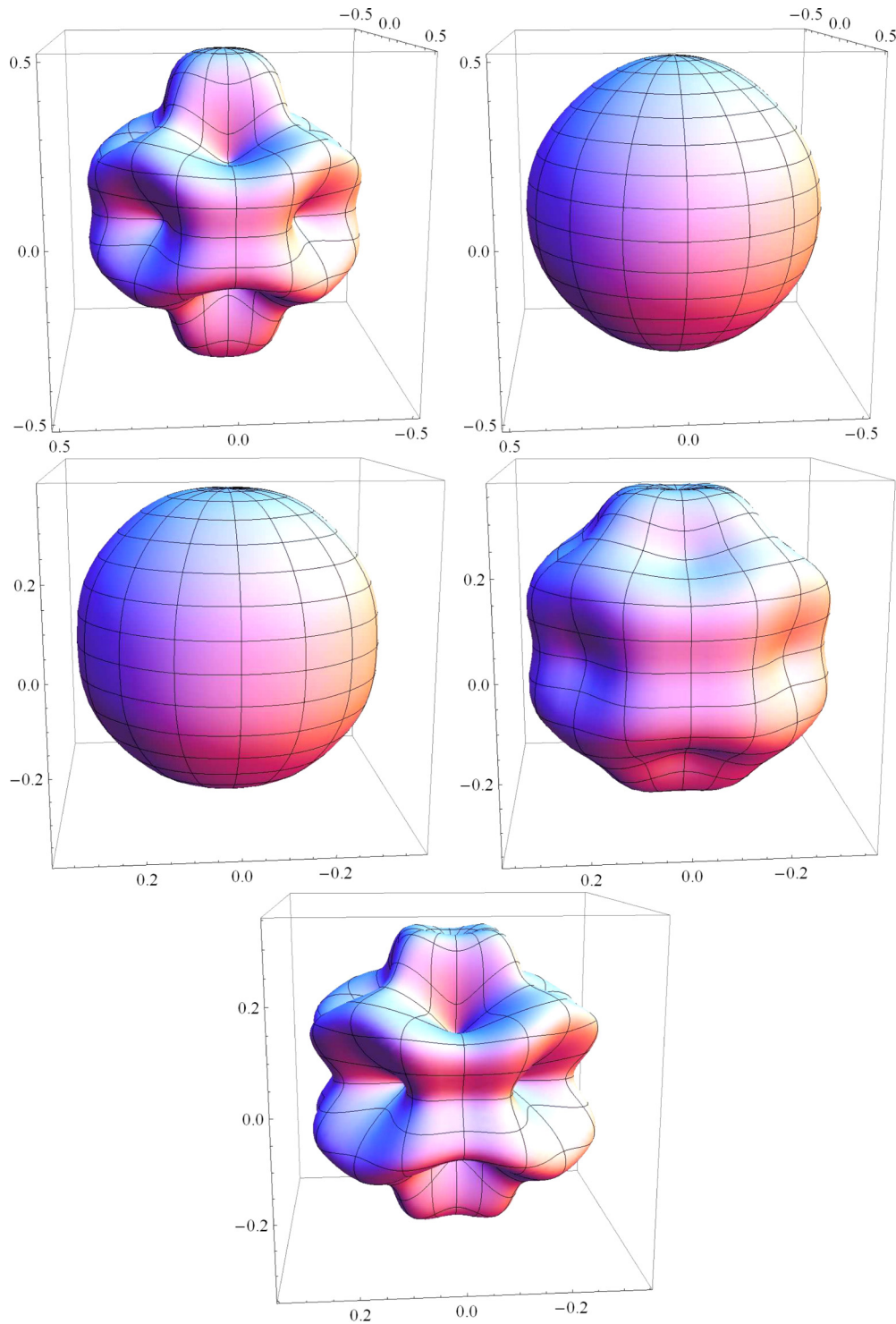


FIG. 14. Calculated energy gradient modula of alkali metals. (The order of the elements as in Fig. 13.)

have only one active electron band. As follows from Sec. III for diamagnetic susceptibility one needs two very important characteristics: the Fermi surface and the energy gradient $\nabla_{\vec{k}}E$ on it. Therefore, we first have performed *ab initio* density functional theory (DFT) calculations of the alkali metals using the Moscow-FLAPW code [31]. The Perdew-Burke-Ernzerhof (PBE) [32] variant of the generalized gradient approximation has been employed, with the number of k points 2470. For the Fermi surface and gradient calculations

we have used the tetrahedron method [33]. In this method the irreducible part of the Brillouin zone is divided into a set of tetrahedra and within each tetrahedron the linear dependence of the band energy $E(\vec{k})$ is assumed. The cross sections of the constant energy $E = E_F$ in the \vec{k} space from all relevant tetrahedra give the pieces forming the Fermi surface. Also, in each tetrahedron crossing the Fermi surface we find the value of the energy gradient, $\nabla_{\vec{k}}E$, which is unchanged within the tetrahedron.

The obtained Fermi surfaces (FS) are shown in Fig. 13. The important property of the calculated Fermi surfaces is that the topological space inside each of them is simply (or path) connected. In other words, the occupied electron states form a single-piece Fermi surface. (The application of the presented method to more complicated Fermi surfaces and to completely filled electron bands requires additional considerations.)

Since the Fermi surface is invariant under all symmetry operations of the crystal (in our case we deal with the O_h cubic symmetry), it can be expanded in terms of symmetry-adapted functions (SAFs) belonging to the fully symmetric (A_{1g}) representation of O_h [34]. Such SAFs, known as cubic harmonics [34], are linear combinations of real spherical harmonics $Y_l^{m,\tau}$ [where $\tau = c, s$ stands for the azimuthal dependence of the cosine (c) or sine (s) type] with $l = 4, 6, 8, \dots$:

$$\begin{aligned} K_4(\theta, \phi) &= \sqrt{\frac{7}{12}} Y_4^0 + \sqrt{\frac{5}{12}} Y_4^{4,c}, \\ K_6(\theta, \phi) &= \sqrt{\frac{1}{8}} Y_6^0 - \sqrt{\frac{7}{8}} Y_6^{4,c}, \\ K_8(\theta, \phi) &= \sqrt{\frac{33}{64}} Y_8^0 + \sqrt{\frac{7}{48}} Y_8^{4,c} + \sqrt{\frac{65}{192}} Y_8^{8,c}. \end{aligned}$$

Here $(\theta, \phi) = \hat{k}$ are polar angles in k space and for spherical harmonics we use the phase convention of Bradley and Cracknell [34]. [For compactness here and below we omit (θ, ϕ) in $Y_l^{m,\tau}$.] Therefore, the Fermi surface can be very accurately represented by the expansion

$$k_F(\hat{k}) = C_0^{FS} Y_0^0 + C_4^{FS} K_4(\hat{k}) + C_6^{FS} K_6(\hat{k}) + C_8^{FS} K_8(\hat{k}), \quad (56)$$

where $Y_0^0 = 1/\sqrt{4\pi}$ is the zeroth spherical harmonic ($l = m = 0$). In the expansion (56) the Fermi surface is completely defined by the coefficients C_0^{FS} , C_4^{FS} , C_6^{FS} , and C_8^{FS} . These coefficients can be obtained numerically from the calculated Fermi surfaces, Fig. 13. For all alkalis they are given in Table I.

The other quantity—energy gradient at the Fermi surface $\vec{\nabla}_k E_F(\hat{k})$ —also can be expanded in terms of the cubic harmonics, Eq. (56). Since the gradient is always normal to the Fermi surface and therefore its direction can be found at any point of the Fermi surface, we need only its modulus expansion,

$$|\vec{\nabla}_k E_F(\hat{k})| = C_0^g Y_0^0 + C_4^g K_4(\hat{k}) + C_6^g K_6(\hat{k}) + C_8^g K_8(\hat{k}). \quad (57)$$

The coefficients C_0^g , C_4^g , C_6^g , and C_8^g obtained from the *ab initio* calculations are also quoted in Table I. The three-dimensional picture of $|\vec{\nabla}_k E_F(\hat{k})|$ as a function of the direction \hat{k} in k space is shown in Fig. 14.

From Fig. 13 and the values of the coefficients C_l^{FS} we conclude that the Fermi surfaces of lithium and cesium demonstrate the largest deformations from the spherical shape. Sodium and potassium, on the other hand, have FS shapes which are very close to spherical, while deviations for rubidium lie between these two groups. This finding is even more clearly illustrated by the shape of energy gradients,

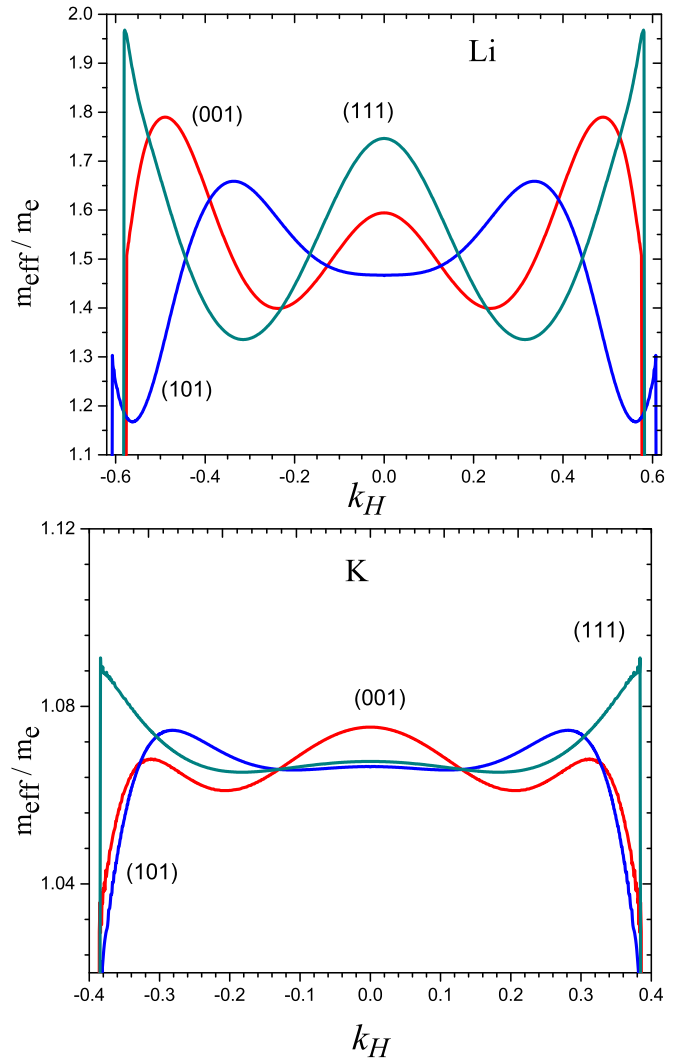


FIG. 15. Calculated cyclotron mass m^* for Li and K for directions [001], [101], and [111] of the magnetic field H .

Fig. 14, which are more sensitive to deviations from the spherical form.

We now study the cyclotron mass m^* , which depends on the closed orbit on the Fermi surface in k space, Eqs. (44), (45). The orbit is given by the cross section of the Fermi surface with a plane lying perpendicular to the applied magnetic field \vec{H} . Such a plane is uniquely defined by its projection $k_H \equiv k_{z'}$ on the z' axis parallel to \vec{H} . Therefore, the cyclotron mass in the applied magnetic field is a function of k_H and \hat{H} pointing in the direction of \vec{H} , that is, $m^* = m^*(\hat{H}, k_H)$. In Fig. 15 we plot m^* as a function of k_H for three directions of magnetic field for potassium with nearly spherical Fermi surface and lithium with a deformed Fermi surface.

Notice that for deformed Fermi surfaces (lithium and cesium) k_H^{\max} and $k_H^{\min} = -k_H^{\max}$ are noticeably different for various directions of H , Table I. In Table I we also quote average cyclotron masses (m_{av}^*) for magnetic field directions [001], [101], and [111], defined according to the following relation,

$$\frac{1}{m_{av}^*} = \frac{1}{|k_H^{\max} - k_H^{\min}|} \int_{k_H^{\min}}^{k_H^{\max}} \frac{dk_H}{m^*(k_H)}. \quad (58)$$

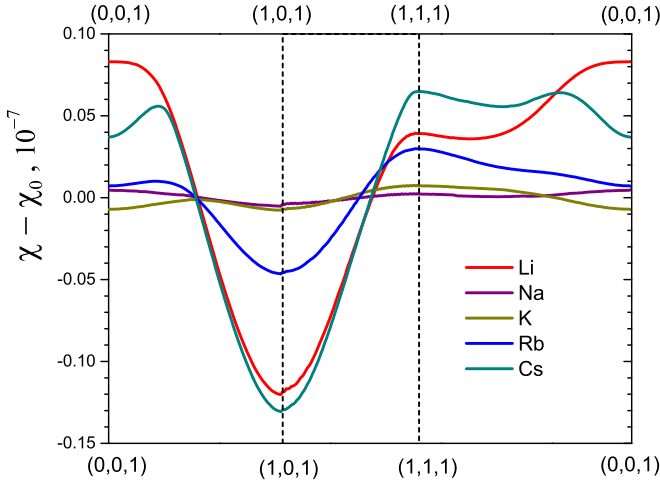


FIG. 16. Calculated deviations of the Landau diamagnetic susceptibility χ_L from its average value χ_L^{av} for various directions of the applied magnetic field H for alkali metals.

Since in general m_{av}^* depends on \hat{H} , the Landau diamagnetic susceptibility χ_L defined by Eq. (55) also shows this dependence. Therefore, to obtain the averaged value χ_L^{av} for each element we perform an effective integration of $\chi_L(\hat{H})$ over \hat{H} , using a special set of 170 points [35]. (The set gives the correct coefficients of expansion up to spherical harmonics with $l = 10$.) The calculated averaged values of χ_L^{av} and m_{av}^* are given in Table I. They are in fair correspondence with estimations of the Landau contributions obtained with other approaches [36].

For a chosen direction of magnetic field \hat{H} , χ_L in general differs from the average value χ_L^{av} , and we can study $\chi_L - \chi_L^{av}$ as a function of \hat{H} . These dependencies for all alkali metals are presented in Fig. 16, where in addition to the selected directions ([001], [101], and [111]) we give data for intermediate angles (i.e., lying on the circumferences fusing [001] and [101], [101] and [111], [111] and [001]). Notice that the deviations from χ_L^{av} are larger for lithium and cesium and smaller for sodium and potassium. The anisotropy of χ_L with respect to the direction of the applied magnetic field is a remarkable property of the Landau diamagnetism, which singles it out from the Pauli paramagnetism and the Langevin diamagnetism of closed electron shells.

V. CONCLUSIONS

The steady diamagnetic response for the Fermi gas and a real metal with a general simply connected Fermi surface is obtained analytically at zero temperature ($T = 0$) within the widely accepted semiclassical approach [2–4,26,27]. The diamagnetic effect is caused by electron states in a very narrow region of the Fermi surface. The consideration is based on a structure in \vec{k} space called a magnetic tube, which sandwiches the Landau level inside it. The completely occupied tubes are diamagnetically inert. Only partially occupied tubes located at the Fermi surface are responsible for the diamagnetic effect. Although energy gradients at the Fermi surface change in the magnetic field, the total density of electron states at the Fermi energy remains constant, Appendix F.

We have applied the method for calculations of the Landau diamagnetic susceptibility χ_L of alkali metals (Li, Na, K, Rb, Cs). The crucial quantities for that are the Fermi surface $k_F(\hat{k})$ and energy gradients $\vec{\nabla}_k E_F(\hat{k})$ on it, which are obtained from *ab initio* band structure calculations. For accurate calculations of χ_L , we expand both $k_F(\hat{k})$ and $|\vec{\nabla}_k E_F(\hat{k})|$ in terms of symmetry-adapted functions, Eqs. (56) and (57). We have demonstrated that the diamagnetic effect depends on the direction \hat{H} of the applied magnetic field \vec{H} . The anisotropy of χ_L is larger for lithium and cesium and smaller for sodium and potassium. It is worth noting that the Langevin diamagnetism of atomic closed core shells and the Pauli paramagnetism are isotropic with respect to \hat{H} .

The present approach can be applied to other metals or intermetallic compounds. The method can also be extended to the case of nonzero temperatures, where the thermal excitations of a one-dimensional electron gas consisting of electron states on the Landau levels should be taken into account.

While the steady response is due to the region just below the Fermi surface, the oscillatory behavior of energy and magnetic susceptibility arises from a few partially occupied tubes located at its extremal cross sections. A small oscillatory change of the Fermi energy of the free electron gas in the applied magnetic field is caused by a transfer (inflow or outflow) of electrons from this equatorial region of the Fermi surface, Sec. IID.

ACKNOWLEDGMENT

I am grateful to the anonymous referee for drawing my attention to Refs. [14] and [11].

APPENDIX A: CALCULATION OF Δk_\perp , Δk_z , ΔN

Here we note some useful relations in a partially occupied tube shown in Fig. 11, taking into account the infinitesimal properties of its triangular (k_z, e_{k_\perp}) cross section. In particular, we have

$$\Delta k_\perp = \frac{\hbar\omega}{|\partial E/\partial k_\perp|} > 0. \quad (\text{A1})$$

To calculate Δk_z we first consider the area A of the (k_x, k_y) cross section of the Fermi surface as a function of k_z , that is, $A(k_z)$. Then $\Delta A = A_{n+1}^{\text{aux}} - A_n^{\text{aux}} = [\partial A(k_z)/\partial k_z]\Delta k_z$, and we arrive at

$$\Delta k_z = \frac{2\pi eH}{c\hbar} \frac{1}{|\partial A/\partial k_z|} > 0. \quad (\text{A2})$$

For the number of the electron states in the partially occupied tube n , Fig. 11, we find

$$\Delta N = 2v \oint_{O_{n+1}} \Delta S dk = v \Delta k_z \oint_{O_{n+1}} \Delta k_\perp dk = v \Delta A \Delta k_z, \quad (\text{A3})$$

where $v = V/(2\pi)^3$ and ΔS is the area of the (k_z, e_{k_\perp}) cross section: $\Delta S = \Delta k_\perp \Delta k_z/2$. This gives Eqs. (17) and (52).

APPENDIX B: CALCULATION OF $\Delta E^{H=0}$, $\Delta E_{\perp}^{H \neq 0}$, $\Delta E_z^{H \neq 0}$

We first consider the energy of a partially occupied tube n without magnetic field ($H = 0$), left panel of Fig. 12. The reference energy at $\vec{k}(R)$ is $E_{\text{ref}} = E(\vec{k}(R)) = E_F - \hbar\omega$, Fig. 11. We will calculate the energy by integrating over x from R to R' along the energy gradient direction $\partial E/\partial \vec{k}|_F$, Fig. 11. Notice that $O'_n O'_{n+1}$ is perpendicular to RR' , the energy at x is $(x/\Delta k_F)\hbar\omega$, and the infinitesimal volume element is $dk dx(x/\Delta k_F)|O'_n, O'_{n+1}|$. Denoting $\Delta l_F = |O'_n, O'_{n+1}|$, we get

$$\Delta E^{H=0} = 2v \oint_{O_{n+1}} \epsilon dk, \quad (\text{B1})$$

where

$$\epsilon = \int_0^{\Delta k_F} \left(\frac{x}{\Delta k_F} \hbar\omega \right) \left(\frac{x}{\Delta k_F} \Delta l_F \right) dx. \quad (\text{B2})$$

Performing integration in (B2) and taking into account that the area of the cross section shown in Fig. 11 is $\Delta S = \Delta k_F \Delta l_F/2$ whereas $2v \oint \Delta S dk = \Delta N$, we arrive at Eq. (23).

We now consider the case $H \neq 0$, the right panel of Fig. 12. The transverse component of an electron state condensed on the Landau level is $E(L) = E_{\text{ref}} + \hbar\omega/2$. Thus, for each electron state we have $\Delta E_{\perp}^{H \neq 0} = \hbar\omega/2$, and for all electron states we obtain Eq. (24a).

Populating the Landau levels along the L, L' line shown in Fig. 11, the one-dimensional electron energy changes from E_{ref} to $E_{\text{ref}} + \hbar\omega/2$. Since in the infinitesimal cross-section approximation of Fig. 11 the energy increases linearly with k_z and the density of electron states along the L, L' line is constant, for the energy of all these occupied states we obtain $\Delta E_z^{H \neq 0} = (\hbar\omega/4) \Delta N$, Eq. (24b).

APPENDIX C: POLAR REGION

If the energy gradient at a certain point P of the Fermi surface is parallel to the z axis (or to the magnetic field \vec{H}), that is, $\partial E(P)/\partial \vec{k} \parallel \vec{H}$, then $[\partial E(P)/\partial \vec{k}]_{\perp} = 0$, but on the other hand, the contour path for $E = E(P)$ in Eq. (45) reduces to the point P . This leads to the ambiguity for $\partial A/\partial E$ in Eq. (45) and consequently for m^* and ω in Eqs. (44) and (43). This situation corresponds to a polar region around the point P and requires a special treatment.

For convenience we put the origin of the coordinate system at the point P and assume that the center of curvature is located below. The Fermi surface in the vicinity of P is given by the function $k_z^{FS}(k_x, k_y) = f(k_x, k_y)$, whose tensor of the second derivatives is diagonalized:

$$\left. \frac{\partial^2 k_z^{FS}}{\partial k_x^2} \right|_P < 0, \quad \left. \frac{\partial^2 k_z^{FS}}{\partial k_y^2} \right|_P < 0, \quad \left. \frac{\partial^2 k_z^{FS}}{\partial k_x \partial k_y} \right|_P = 0. \quad (\text{C1})$$

This polar region of the Fermi surface is described by the function

$$k_z^{FS}(k_x, k_y) = \frac{1}{2} \left. \frac{\partial^2 k_z^{FS}}{\partial k_x^2} \right|_P k_x^2 + \frac{1}{2} \left. \frac{\partial^2 k_z^{FS}}{\partial k_y^2} \right|_P k_y^2. \quad (\text{C2})$$

In the polar region we deal with the zeroth magnetic tube, i.e., $n = 0$, and with the zeroth Landau level. Two tubes' auxiliary boundary conditions are reduced to

$$A_{n=0}^{\text{aux}} = 0, \quad (\text{C3a})$$

$$A_1^{\text{aux}} = \frac{2\pi eH}{\hbar c}. \quad (\text{C3b})$$

(Notice that here $\delta = 0$.) Thus, the first quantized auxiliary orbit $O_{n=1}$ at the Fermi surface is an ellipse at $\Delta k_z = k_{z,1} < 0$, which can be found by equating its area to A_1^{aux} , Eq. (C3b). The result is

$$\Delta k_z = -\frac{eH}{\hbar c} \sqrt{\left. \frac{\partial^2 k_z^{FS}}{\partial k_x^2} \right|_P \left. \frac{\partial^2 k_z^{FS}}{\partial k_y^2} \right|_P}. \quad (\text{C4})$$

Therefore, the whole polar region with $0 \geq k_z \geq \Delta k_z$ represents the zeroth partially occupied tube. It can be shown that the volume of the polar region is

$$V_P = \frac{1}{2} |\Delta k_z| A_1^{\text{aux}}. \quad (\text{C5})$$

The same expression holds for a small sphere cap in the case of the Fermi sphere of the free electron gas. The number of active electron states ($\vec{H} = 0$) is then

$$\Delta N_{n=0} = 2v V_P = |\Delta k_z| \frac{2\pi eH}{\hbar c} v. \quad (\text{C6})$$

The latter equation demonstrates that $\Delta N_0/|\Delta k_z|$ follows the general relation (52) although the curvature of the Fermi surface polar region has been explicitly taken into account. Analogously, one can show that the other quantities (energy, etc.) also follow the general consideration.

APPENDIX D: TUNING AUXILIARY BOUNDARY CONDITIONS

In this section we will give details of derivation of Eqs. (50) and (51b) and define the small parameter $\delta \sim H$ in Eq. (47). The middle part of Eq. (50) can be integrated by parts,

$$\begin{aligned} \mathcal{E}_n(H=0) &= 2 \frac{L_x L_y}{(2\pi)^2} \left[E_{n+1}^{\text{aux}} A_{n+1}^{\text{aux}} - E_n^{\text{aux}} A_n^{\text{aux}} - \int_{E_n^{\text{aux}}}^{E_{n+1}^{\text{aux}}} A(E) dE \right]. \end{aligned} \quad (\text{D1})$$

Introducing notations $\Delta E = E_{n+1}^{\text{aux}} - E_n^{\text{aux}}$, $\Delta A = (2\pi e/c\hbar)H$, Eq. (D1) can be written as

$$\mathcal{E}_n = [E_{n+1}^{\text{aux}}(1 - \Delta^* + \delta) + E_n^{\text{aux}}(\Delta^* - \delta)] \Delta N_n, \quad (\text{D2})$$

where

$$\Delta^* = \frac{1}{\Delta A \Delta E} \int_{E_n^{\text{aux}}}^{E_{n+1}^{\text{aux}}} A(E) dE - n. \quad (\text{D3})$$

We further expand $A(E)$ up to the second derivative term,

$$A(E) = A(E_0) + A'(E - E_0) + \frac{1}{2} A''(E - E_0)^2, \quad (\text{D4})$$

where $E_0 = (E_{n+1}^{\text{aux}} - E_n^{\text{aux}})/2$ and we use short notations $A' = \partial A(E_0)/\partial E$, $A'' = \partial^2 A(E_0)/\partial E^2$. With Eq. (D4) we

obtain

$$\Delta^* = \frac{1}{2} + \delta - \frac{A''(\Delta E)^2}{12 \Delta A} + O(H^3), \quad (\text{D5})$$

where $O(H^3) \sim H^3$ and Eq. (D2) becomes

$$\mathcal{E}_n(H=0) = \left[E_0 + \frac{A''(\Delta E)^2}{12 \Delta A} \right] \Delta N_n. \quad (\text{D6})$$

On the other hand, for the energy of the tube in the magnetic field with respect to E_0 one has

$$\mathcal{E}_n(H \neq 0) = \left[E_0 - \frac{\Delta A}{A'} \delta + \frac{1}{8} \frac{A''}{A'} (\Delta E)^2 \right] 2N_p. \quad (\text{D7})$$

Equating Eqs. (D6) and (D7), we obtain

$$\delta = \frac{\pi e}{12c\hbar} \frac{A''}{(A')^2} H. \quad (\text{D8})$$

If, as in Eq. (5), one uses $\gamma = 1/2 + \Gamma_1 h$ [27], then in Eq. (D8) δ should be replaced with $(\delta - \gamma) \sim H$. From Eq. (D8) it follows that δ is also a function of energy, $\delta = \delta(E)$. This in turn leads to a more complicated final expression,

$$\delta(E) = \frac{\pi e}{12c\hbar} \frac{f(E)}{[1 + Ef'(E)/f(E)]} H, \quad (\text{D9})$$

which can be solved iteratively, starting with $f_0(E) = A''(E)/A'(E)^2$ as in Eq. (D8).

Quantities γ and δ should be taken into account for the definition of the boundaries of the occupied magnetic tubes, because they concern a large number of electron states inside the Fermi surface. For partially occupied tubes at the Fermi surface they give only small corrections on the order of $\hbar\omega/E_F$ to the main results, which can be omitted.

APPENDIX E: CONNECTION WITH PEIERLS' EXPRESSION

In his early pioneer work [8], Peierls obtained Eq. (2) for the steady diamagnetic susceptibility. Below we will show that the magnetic susceptibilities given by Eqs. (2) and (55) coincide for the case of the parabolic energy band dependence in terms of k_x and k_y ,

$$E(\vec{k}) = a(k_z)k_x^2 + b(k_z)k_y^2 + c(k_z)k_x k_y + d(k_z). \quad (\text{E1})$$

Notice that $a(k_z)$, $b(k_z)$, $c(k_z)$, $d(k_z)$ here are arbitrary smooth functions of k_z and the z axis points in the direction of the applied magnetic field H . The expression in the curly bracket of Eq. (2), being $\lambda = 4ab - c$, is an invariant of the quadratic form (E1). We then transform (E1) to a new coordinate system (k'_x, k'_y) where it takes the diagonal form $E(\vec{k}) = a'(k_z)k_x'^2 + b'(k_z)k_y'^2 + d(k_z)$. Now $\lambda = 4a'b'$ and in the following will work in this representation. For the integral in Eq. (2) we obtain

$$\begin{aligned} I &= -4 \int_{FS} \frac{a'(k_z)b'(k_z)dS(\vec{k})}{|\nabla_{\vec{k}} E(\vec{k})|} \\ &= 4\pi \int_{k_z^{\min}}^{k_z^{\max}} \sqrt{a'(k_z)b'(k_z)} dk_z, \end{aligned} \quad (\text{E2})$$

where the first integration is taken over the Fermi surface (FS) and k_z^{\max} (k_z^{\min}) is the maximal (minimal) projection of the FS on the z axis. The final expression for Eq. (2) becomes

$$\chi = -\frac{e^2}{12\pi^2 \hbar^2 c^2} \int_{k_z^{\min}}^{k_z^{\max}} \sqrt{a'(k_z)b'(k_z)} dk_z. \quad (\text{E3})$$

On the other hand, using Eq. (44) we obtain $m^*(k_z) = \hbar^2/2\sqrt{a'(k_z)b'(k_z)}$. Substitution of $m^*(k_z)$ in Eq. (55) gives the same result as before, Eq. (E3).

In general however Eq. (2) differs from Eq. (55). We ascribe it to a number of approximations used in the derivation of Eq. (2) [11,13,14].

APPENDIX F: DENSITY OF ELECTRON STATES AT E_F

Consider the partitioning of the Fermi surface region in partially occupied tubes. The density of electron states (DOS) at the Fermi energy then is given by

$$g(E_F) \frac{1}{V} = \sum \Delta g_n(E_F) = \int_{k_{z,\min}}^{k_{z,\max}} dk_z \frac{\Delta g(E_F)}{\Delta k_z}, \quad (\text{F1})$$

where $\Delta g_n(E_F)$ is the DOS contribution from the part of the Fermi surface S_n associated with a partially occupied tube n ,

$$\Delta g_n(E_F) = \frac{1}{4\pi^3} \oint_{S_n} \frac{dS}{|\nabla E|}. \quad (\text{F2})$$

In the applied magnetic field $H \neq 0$, Fig. 11, electron states occupy the Landau level n along the L, L' line. Since the Landau orbits are perpendicular to the z axis, the energy gradient should be taken in the z direction with the surface element dS in the (k_x, k_y) plane. From Fig. 11 we obtain $\partial E/\partial k_z = \hbar\omega/\Delta k_z$, $dS_{\perp} = \Delta k_{\perp} dk$. We thus arrive at

$$\Delta g^{H \neq 0}(E_F) = \frac{1}{4\pi^3} \oint \frac{\Delta k_{\perp} \Delta k_z}{\hbar\omega} dk. \quad (\text{F3})$$

Notice that $\Delta S = \Delta k_{\perp} \Delta k_z/2$ is the area of the triangular (O'_n, A, O'_{n+1}) cross section, which can also be written as $\Delta S = \Delta k_F \Delta l_F/2$. Since $|\partial E/\partial \vec{k}| = \hbar\omega/\Delta k_F$, we continue Eq. (F3) as

$$\Delta g^{H \neq 0}(E_F) = \frac{1}{4\pi^3} \oint \frac{\Delta l_F dk}{|\partial E/\partial \vec{k}|} = \Delta g^{H=0}(E_F). \quad (\text{F4})$$

Here in establishing the last equality we have taken into account that $\Delta l_F dk = dS^{H=0}$ is a part of the Fermi surface perpendicular to the energy gradient $\partial E/\partial \vec{k}$ in the absence of the magnetic field. Equation (F4) leads to $g^{H \neq 0}(E_F) = g^{H=0}(E_F)$.

- [1] L. Landau, *Z. Phys.* **64**, 629 (1930); L. D. Landau and E. M. Lifshitz, *Statistical Physics* (Pergamon, Bristol, 1995), Vol. 5.
- [2] L. Onsager, *Philos. Mag.* **43**, 1006 (1952).
- [3] A. M. Kosevich and I. M. Lifshits, *Zh. Eksp. Teor. Fiz.* **29**, 743 (1956) [*Sov. Phys. JETP* **2**, 646 (1956)]; M. I. Kaganov and I. M. Lifshits, *Usp. Fiz. Nauk* **129**, 487 (1979) [*Sov. Phys. Usp.* **22**, 904 (1979)].
- [4] D. Shoenberg, *Magnetic Oscillations in Metals* (Cambridge University Press, London, 1984).
- [5] N. W. Ashcroft and N. D. Mermin, *Solid State Physics* (Brooks/Cole, 1976).
- [6] J. Callaway, *Quantum Theory of the Solid State*, Part B (Academic, 1974).
- [7] P. K. Misra and L. M. Roth, *Phys. Rev.* **177**, 1089 (1969).
- [8] R. Peierls, *Z. Phys.* **80**, 763 (1933).
- [9] A. H. Wilson, *Theory of Metals* (Cambridge University Press, 1936).
- [10] J. E. Hebborn and E. H. Sondheimer, *J. Phys. Chem. Solids* **13**, 105 (1960).
- [11] P. Briet, H. D. Cornean, and B. Savoie, *Ann. Henri Poincaré* **13**, 1 (2012).
- [12] A. H. Wilson, *Proc. Cambridge Philos. Soc.* **49**, 292 (1953).
- [13] E. N. Adams, *Phys. Rev.* **89**, 633 (1953).
- [14] T. Kjeldaa, Jr. and W. Kohn, *Phys. Rev.* **105**, 806 (1957).
- [15] E. Brown, in F. Seitz, D. Turnbull, and H. Ehrenreich, editors, *Solid State Physics: Advances in Research and Applications*, Vol. 22 (Academic Press, New York, 1968), p. 313.
- [16] L. M. Roth, *J. Phys. Chem. Solids* **23**, 433 (1962).
- [17] E. I. Blount, *Phys. Rev.* **126**, 1636 (1962).
- [18] G. H. Wannier and U. N. Upadhaya, *Phys. Rev.* **136**, A803 (1964).
- [19] A. G. Samoilovich and E. Ya. Rabinovich, *Sov. Phys. Solid State* **5**, 567 (1963).
- [20] M. L. Glasser, *Phys. Rev.* **134**, A1296 (1964).
- [21] F. A. Butler and E. Brown, *Phys. Rev.* **166**, 630 (1968).
- [22] G. E. Zil'berman, *Zh. Eksp. Teor. Fiz.* **32**, 296 (1957) [*Sov. Phys. JETP* **5**, 208 (1957)].
- [23] J. E. Hebborn and N. H. March, *Adv. Phys.* **19**, 175 (1970).
- [24] T. Holstein, R. E. Norton, and P. Pincus, *Phys. Rev. B* **8**, 2649 (1973).
- [25] A. M. Tselik *Quantum Field Theory in Condensed Matter Physics*, 2nd ed. (Cambridge University Press, Cambridge, 2003).
- [26] M. Brack and R. K. Bhaduri, *Semiclassical Physics* (Addison-Wesley Publishing, 1997).
- [27] L. M. Roth, *Phys. Rev.* **145**, 434 (1966).
- [28] N. A. Zimbovskaya, *Local Geometry of the Fermi Surface* (Springer Science and Business Media, New York, 2001).
- [29] M. I. Kaganov, I. M. Lifshitz, and K. D. Sinel'nikov, *Zh. Eksp. Teor. Fiz.* **32**, 605 (1957) [*Sov. Phys. JETP* **5**, 500 (1957)].
- [30] A. B. Pippard, *Rep. Prog. Phys.* **23**, 176 (1960).
- [31] A. V. Nikolaev, D. Lamoen, and B. Partoens, *J. Chem. Phys.* **145**, 014101 (2016).
- [32] J. P. Perdew, K. Burke, and M. Ernzerhof, *Phys. Rev. Lett.* **77**, 3865 (1996).
- [33] G. Lehmann and M. Taut, *Phys. Status Solidi B* **54**, 469 (1972).
- [34] C. J. Bradley and A. P. Cracknell, *The Mathematical Theory of Symmetry in Solids* (Clarendon, Oxford, 1972).
- [35] V. I. Lebedev, *Comput. Math. Math. Phys.* **16**, 10 (1976); V. I. Lebedev and D. N. Laikov, *Dokl. Math.* **59**, 477 (1999).
- [36] C. Oliver and A. Myers, *J. Phys.: Condens. Matter* **1**, 9457 (1989).